UCRL-ID-124115

The Inductrack Concept: a New Approach to Magnetic Levitation

Richard F. Post and Dmitri Ryutov

May, 1996

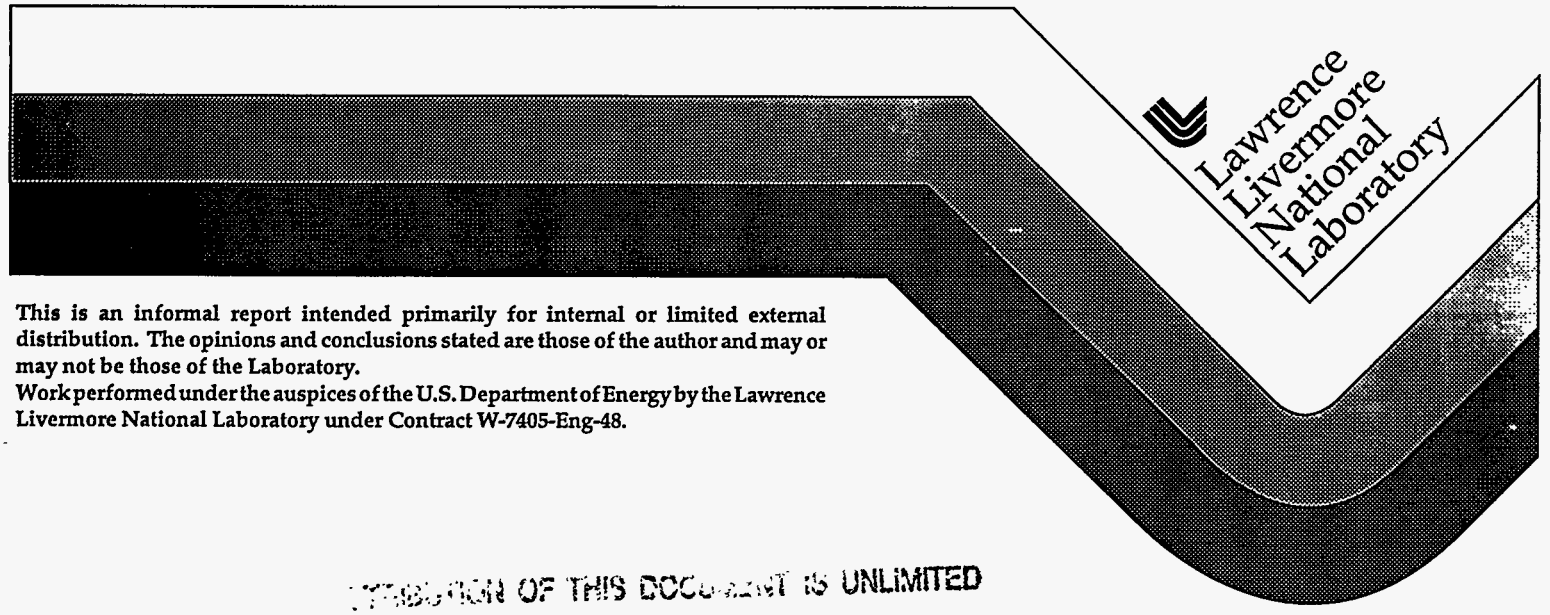

DISCLAIMER

The Inductrack Concept: a New Approach to Magnetic Levitation

Richard F. Post and Dmitri D. Ryutov

Table of Contents

List of notations

a - radius (m.) of a single wire of which the track conductors are made

A - x-component of the vector-potential

B - magnetic field (Tesla)

B_0- amplitude value of the magnetic field on the surface of the track

B_r - remanent magnetic field of the permanent magnets

d - distance between the tower and upper side of the Halbach array

d_c- width of a conductor (in the direction of track)

f - filling factor of the winding (fraction of the winding occupied by metal)

F_y - lifting force (Newtons)

F_z - drag force

h - the distance between the upper and the lower legs of the circuit

I - current in an individual circuit (amperes)

j - current density (amperes/m^2)

k - wave-number of the Halbach array ($k=2\pi/\lambda$)

K - the ratio of the lifting force to the power loss (Newtons/Watt)

L - lumped self-inductance associated with every conductor (Henrys)

$L^{(d)}$-distributed inductance

L_{car}-length of the car

M - number of magnet bars per wavelength of the Halbach array (section IVA); mass of the car (Appendix 6)

P - dissipated power (Watts)

P_c - perimeter of the circuit (in the vertical plane)

R - resistance of the individual circuit of the track (ohms)

v - speed of the car (m./sec.)

V - electromotive force produced by the external source in the circuit (Volts)

w - the width of the Halbach array

y_1 - the distance between the track and the lower side of the Halbach array

Δ_c - vertical thickness of the conductor

β - number of circuits per quarter-wavelength

γ- dimensionless thickness of the coil ($\gamma=\lambda/4\Delta_c$)

δ - skin-depth

λ – spatial period of the Halbach array

μ_0 - permeability of free space ($4\pi \times 10^{-7}$ hy/meter)

ϕ - magnetic flux of permanent magnets enclosed by an individual circuit

ϕ_0 - amplitude value of the same quantity

ρ – resistivity of the conductor (ohm-meters)

ω - frequency of the magnetic field variations in the track frame (ω =kv) (radians/sec.)

I) Introduction

This report describes theoretical and experimental investigations of a new approach to the problem of the magnetic levitation of a moving object. By contrast with previously studied levitation approaches, the Inductrack concept represents a simpler, potentially less expensive, and totally "passive" means of levitating a high-speed train. It may also be applicable to other areas where simpler magnetic levitation systems are needed, for example, high-speed test sleds for crash-testing applications, or low-friction conveyor systems for industrial use.

In present maglev train systems [1], test tracks of which have been built in Germany and Japan, the train cars are levitated by the use of electromagnets that are energized so as to produce a lifting force against a specially designed ferromagnetic track. In such situations Earnshaw's Theorem dictates that the levitated system (the train car) will be unstable against vertical displacements. Thus it is necessary to employ sophisticated sensors and control circuitry in order to maintain the train in a levitated state at the proper height above the track, independent of speed. Failure of these control systems could lead to serious consequences, so that high reliability is required. Energizing the magnets also requires an on-board source of power of high reliability and non-trivial power level, an additional complication.

It would be highly desirable if a passive levitation system could be employed, one that relied only on the kinetic motion of the train to produce its levitating force, and one for which the consequences of a failure of the source of driving power leads to a benign failure in the levitation. While some earlier approaches to passive levitation [2] aimed at a similar objective, they involved substantial power losses to achieve levitation. These power losses are both on board in the train (to refrigerate superconducting magnets) and in the track itself (eddy current losses in sheet conductors). The present proposal aims at accomplishing passive

levitation with zero on-board power requirements and minimal track losses. It also aims at a system that efficiently combines both passive levitation and electric propulsion means in the same track structure.

II) Technical Aspects

The concept to be explored here involves the following two main components:

- One or more arrays of permanent magnets on the moving object, producing a spatially periodic magnetic field below each array.

- A "track" made up of a close-packed array of inductively loaded circuits embedded in the surface of the track.

At rest ("in the station") no levitation occurs and the train car relies on auxiliary wheels to carry its weight. However as soon as it is in motion at an appreciable speed (a few kilometers per hour) the moving magnet array will induce currents in the conductor array and thereby levitate the train. Owing to the inductive loading of the circuits (self-inductance, plus the effect of mutual inductances) the phase of the induced current is shifted by ninety degrees, thus maximizing the lift force, while minimizing the drag force. As a result, in a high-speed train the drag power can be made to be a small fraction of the power required to overcome aerodynamic friction (in an example, of order three percent of the drive power was all that was needed). As long as the train is in motion it will be levitated. Furthermore, theory shows that, for properly chosen shapes of the magnets and the track, the levitation mechanism is stable against both vertical and transverse displacements, independent of speed or load (up to the maximum permitted load of the car). If the driving power fails, the train will simply slow down, and come to rest on its auxiliary wheels as its speed approaches zero. No on-board power or levitation control circuitry is required, and the permanent magnet arrays should have a high degree of reliability.

A preliminary estimate of the cost of a track based on the new concept indicates that it should be not more than, and possibly could be less than, that of the present systems. One reason for this is that, as noted above, it should be possible to incorporate the driving function into the same circuits that are to be employed for levitation,

thus eliminating the need for a separate linear induction motor in the track [3].

Fig. 1 is a schematic representation of the Inductrack concept. Shown in the drawing is the track, made up of a close-packed array of inductively loaded circuits, and the permanent-magnet arrays on a levitated car.

In a theoretical analysis of the concept (discussed in a later section) a very simple approximate expression for the lift-to-drag ratio of the system was derived. From this expression it is easy to show that the drag force actually decreases as the speed increases, by contrast with aerodynamic drag or bearing-friction drag on a conventional train, which always increases with speed. The expression derived is as follows:

$$\frac{Lift}{Drag} = (\omega L / R)$$

Here L (hy) is the inductance of an individual circuit, R (ohms) is the resistance of the circuit, and ω is the angular frequency of the exciting wave. This frequency is in turn determined simply from the spatial wavelength of the permanent magnet array and the speed of the train over the track. Since ω increases directly with speed, above a transition speed (that speed where ω becomes equal numerically to R/L) the lift-to-drag ratio increases linearly with increasing speed, reaching values of order 300:1 at typical operating speeds (compare 25:1 for the typical airfoil of a jet airplane). It is a straightforward matter to adjust the L/R of the circuits so that the lift-to-drag ratio is very large compared to unity at all but the lowest speeds, corresponding to a very low power requirement per kilogram levitated. As a typical number, a levitating parameter of 2.0 Newtons per Watt could be targeted. This corresponds to a levitating power requirement (derived solely from the motion of the car relative to the track) of about 250 kw for an example train car [4] weighing 50,000 kilograms and requiring 8.3 MW to overcome aerodynamic losses at operating speeds (500 kilometers per hour). The calculated levitating power is thus about 3 percent of the drive power at full speed.

III) Outline of Topics

The report consists of three main sections. These cover the following topics:

- A "lumped-circuit" theoretical treatment that defines the main parametric scaling laws for the concept and provides a practical basis for the design of such systems.

- A generalization of the "lumped-circuit" analysis that allows one to take into account effects of inductive interactions of the circuits[1] and also provides a means to evaluate the Inductrack concept against one that provides the maximum possible levitation force from the permanent-magnet array (i.e., by conceptually replacing the inductively loaded circuits in the "track" with a continuous sheet of a perfect conductor).

- A brief discussion of some of the practical and economic issues that can be expected to be encountered in the implementation of the Inductrack concept in full-scale systems.

A discussion of some issues of a more computational nature is presented in Appendices 1-9.

IV) Lumped-Circuit Analysis of the Inductrack

Before beginning the analysis it is necessary to define the geometry of the system being analyzed. Fig. 2 shows schematically one possible form of the circuits in the track. (Other possible configurations will be mentioned later). As can be seen, the circuits resemble window frames, the lower horizontal portions of which are surrounded by ferromagnetic material so as to provide the necessary inductive loading. An appropriate ferromagnetic material would be ordinary transformer laminations (with an air gap to limit the flux

---

[1] Though inductive interaction occurs between many circuits, it turns out that its contibution to the circuit equation can be reduced just to an additional inductance $L^{(d)}$ which is additive to the self-inductance L of every cirquit. The superscript "d" stands for the word "distributed" because the term $L^{(d)}$ describes what can be called "distributed inductance".

density). By appropriately staggering the location of these lamination stacks the circuits could be closely packed together, as shown. The circuits themselves are to be made up of multi-turn windings of multi-strand (litzendraht) wire. The use of multi-turn windings forces the current density to be constant within a conductor bundle; the use of multi-stranded wire minimizes parasitic eddy currents (whose role is quantitatively assessed in Appendix 5).

Beyond the function of providing inductive loading to the circuits, the lamination stacks can fulfill another function, that of coupling in electrical energy to the track in order to propel the car. By threading the lamination stacks with other windings, these stacks become equivalent to transformers, with the Inductrack circuits functioning as their secondary windings. Now, if pulses properly synchronized with the passage of the car are applied to the primary windings, a forward driving force will be exerted on the Halbach array magnets. Braking forces could also be provided in the same manner, by controlling the phase of the driving pulses.

The second major components of the Inductrack system, shown schematically in Fig. 3, are spatially periodic arrays of permanent magnet bars located on the levitated car. We here choose an iron-free array, the "Halbach array" [5], which makes optimal use of the permanent magnet material, maximizing the field below the array, while cancelling out the field above the array. As derived by Halbach (for application of his array to free-electron lasers), simple analytic expressions are available that accurately reproduce the magnetic field produced by such arrays. These expressions will be used in deriving the lift and drag equations.

Many of the salient features of the concept can be obtained from a lumped-circuit type of analysis, one in which the individual circuits are considered to be decoupled electrically from their neighbors, so that the lift and drag forces are calculated by a simple superposition of the forces from each circuit. Simply stated, the main condition that is to be satisfied in order for such an analysis to be valid is that the self-inductance of each circuit should be substantially larger than the mutual inductance between the circuits. In many cases this condition will be well satisfied. In the broader theoretical analysis (Section V) this approximation will not be made, providing a means for correcting the lumped-circuit analysis to include mutual inductance effects.

Another requirement for the simplest equations to apply is that the operating speed should be high compared to the transition speed. That is, it should be high compared to the speed where $\omega=2\pi v/\lambda=R/L$, with v m-sec^{-1} being the speed of the levitated object, and λ m. being the wavelength of the periodic magnet array. Typically the magnitude of R/L corresponds to speeds of one or two kilometers per hour, i.e., very much lower than the operating speed.

An important assumption, one which we use throughout the report, is that the width of the conductors in the direction of motion (z direction), d_c, is small compared to $k^{-1} \equiv \lambda/2\pi$. The significance of this assumption will be highlighted in the appropriate parts of our report.

A. Circuit Equations and the Transition Speed.

The equivalent circuit of one circuit of the Inductrack circuit array is shown in Fig. 4. The circuit equation for this configuration takes the form:

$$V = L\frac{dI}{dt} + RI = \omega\phi_0 \cos(\omega t) \qquad (1)$$

Here I is the induced current and ϕ_0 is the peak flux enclosed by the circuit. (Other terms have been previously defined); V is proportional to the rate of change of flux through the circuit. The flux itself has been taken to vary as sin(ωt). We consider Halbach arrays of sufficient length (many wavelengths) in the direction of motion so that one can neglect transient phenomena and limit oneself to the analysis of steady-state oscillations only.

The steady-state solution of Eq.(1) is:

$$I(t) = \frac{\phi_0}{L}\frac{1}{1+(R/\omega L)^2}\left[\sin(\omega t) + \frac{R}{\omega L}\cos(\omega t)\right] \qquad (2)$$

As can be seen, in the limit $\omega >> R/L$ the phase is shifted 90° with respect to the voltage so that the current is in phase with the flux (that phase which will be seen to correspond to the maximum lifting force). In this limit the expression for the current takes the simple form:

$$I(t) = \frac{\phi_0}{L}\sin(\omega t) \qquad (3)$$

Since we are to calculate the force on a magnet array with a wavelength, λ m., in the z direction, moving at velocity v m. sec^{-1}, we will replace (ωt) by (kz) in equation (3) in calculating the forces, where $k = 2\pi/\lambda$.

Equation (2) can also be seen to provide a rationale for defining the "transition speed" as that speed where $\omega = 2\pi v / \lambda = R/L$.

The coordinate frame that we are going to use throughout this report is shown in Fig. 2: its origin is situated on the upper surface of the track, with axis z pointing in the direction of the car motion along the track, axis y pointing towards the magnet array and axis x pointing across the track. The distance between the track and the lower surface of Halbach array will be denoted by y_1.

To calculate the lift and drag forces we will require expressions for the longitudinal (z) and vertical (y) components of the magnetic field from a Halbach array. To a close approximation these are given by:

$$B_z = B_0 \sin(kz) \exp\left[-k(y_1 - y)\right] \tag{4}$$

$$B_y = B_0 \cos(kz) \exp\left[-k(y_1 - y)\right] \tag{5}$$

where B_0 is the peak strength of the magnetic field at the surface of the Halbach array (i.e., at $y=y_1$). The value of B_0 in terms of the remanent field, B_r, of the permanent magnet material, and the thickness (in the y direction), d m., of the magnet bars is given by the expression [5]:

$$B_0 = B_r\left[1 - \exp(-kd)\right]\frac{\sin(\pi/M)}{\pi/M} \tag{6}$$

Here M is the number of magnet bars per wavelength (4 in the Figure). Some details related to this expression for M=4 are discussed in Appendix 1.

In the case where M = 4 and $d = \lambda/4$ (square magnet bars, as shown in the figure), the value of B_0 is equal to $0.713B_r$. For typical NdFeB (Neodymium-Iron-Boron) commercial-grade magnets the value of B_r is about 1.25 Tesla, so that B_0 = 0.9 T. Recently NdFeB magnet material with B_r values of 1.41 T has become available. If

combined with larger M values (more magnet bars per wavelength) and/or thicker magnet sections, B_0 values in excess of 1.0 Tesla become feasible.

As an index of the levitating power of such fields, a field of 1.0 Tesla in interaction with a conducting surface is capable of levitating about 40,000 kilograms per square meter. An evaluation of the actual levitating forces for the Inductrack system will be derived in what is to follow. The force limit ultimately arises from the constraints imposed by the Maxwell stress tensor of the field. However, it can already be deduced from the estimate given above that modern permanent magnet material can create fields capable of levitating masses that are one to two orders of magnitude larger than the mass of the magnets themselves, auguring well for the economic potential of the Inductrack concept.

An expression for the induced flux, ϕ, can be obtained by integration of equation (4) for B_z over y between the upper and lower legs of the circuit. Thus the integral is to be taken between y=0, the location of the upper leg of the circuit (relative to the lower surface of the Halbach array) and y=-h, where h m. is the distance between the upper and lower legs of the circuit:

$$\phi = \frac{wB_0}{k}\exp(-ky_1)\sin(kz)[1-\exp(-kh)] \qquad (7)$$

In this analysis the circuit is considered to be of negligible thickness in y and z. Later, we will introduce corrections that would allow us to take into account the finite thickness of the track winding.

As for the latter approximation ($d_c << k^{-1}$), this is just the approximation mentioned in the last paragraph before Sec.IVA. It may be called "a quasi-continuous approximation" and is quite significant: Within this approximation, the z-t dependence of the currents in the track follows a simple harmonic law, $A\cos(kz-\omega t)+B\sin(kz-\omega t)$. In the reference frame of a magnet, where $(kz-\omega t)$ is constant, the track currents do not vary with time and, therefore, there are no hysteresis or other losses in the magnets. A coarser segmentation would have two undesirable consequences: first, it would reduce the amplitude of magnetic flux variations through each circuit; second, it would cause the appearance of time-varying

magnetic fields in the car frame and, thereby, introduce a new channel for losses (induced eddy currents).

Typically, the distance between the upper and the lower legs of the circuit, h, is greater than the wavelength, making the exponential term in square brackets of equation (7) very small. Indeed, even for $h=\lambda$ this term is equal to 1/500. In what follows, we will therefore always neglect the terms involving exp(-kh).

Inserting equation (7) into equation (3) for the current (and neglecting the just-mentioned exponentially small terms) one finds for the current in the x direction, $I_x(z)$, the expression:

$$I_x(z) = \frac{\lambda B_0 w}{2\pi L} \frac{1}{1+(R/\omega L)^2} \exp(-ky_1)\left[\sin(kz) + \frac{R}{\omega L}\cos(kz)\right], \text{ amp/circuit} \qquad (8)$$

Here w m. is the width of the magnet bars in the x direction, i.e. transverse to the direction of motion along the track, thus parallel to the direction of the induced current in the track.

This current then interacts with the magnetic field to produce the levitating force (i.e., the force in the vertical (y) direction), and the drag force (i.e., the force in the horizontal (z) direction):

$$F_y = I_x B_z w, \quad F_z = I_x B_y w \qquad \text{N/circuit.} \qquad (9)$$

Averaging this expression over the wavelength one finds the average force to be given by:

$$\langle F_y \rangle = \frac{B_0^2 w^2}{2kL} \frac{1}{1+(R/\omega L)^2} \exp(-2ky_1) \qquad \text{N/circuit} \qquad (10)$$

$$\langle F_z \rangle = \frac{B_0^2 w^2}{2kL} \frac{(R/\omega L)}{1+(R/\omega L)^2} \exp(-2ky_1) \qquad \text{N/circuit} \qquad (11)$$

The fact that the winding has a finite thickness (Δ_c) in the y-direction means, for a uniform distribution of the current in the winding, that the "center of gravity" of this current is situated at a distance $\Delta_c/2$ from the surface of the winding. Thus, in order to obtain a more accurate expression for the forces, one should replace y_1 in equations (10) and (11) by $y_1+(\Delta_c/2)$. A more detailed analysis (which we will not present here) shows that the accuracy of these expressions is

better than 10% if Δ_c is not too large, i.e., if $\Delta_c < 1/(2k)$. These more accurate expressions for the forces then read:

$$\langle F_y \rangle = \frac{B_0^2 w^2}{2kL} \frac{1}{1+(R/\omega L)^2} \exp(-2ky_1 - k\Delta_c) \text{ N/circuit} \qquad (10')$$

$$\langle F_z \rangle = \frac{B_0^2 w^2}{2kL} \frac{(R/\omega L)}{1+(R/\omega L)^2} \exp(-2ky_1 - k\Delta_c) \text{ N/circuit} \qquad (11')$$

In what follows, we will present all results pertinent to multiturn windings in a form analogous to equations (10) and (11), i.e., in the approximation of the zero-thickness winding. The transition to the more accurate expressions can be made in the final results for the forces simply by the substitution that leads from equations (10) and (11) to (10') and (11'), that is, $y_1 \rightarrow y_1 + (\Delta_c/2)$.

The Lift/Drag ratio can be obtained immediately from equations (10) and (11):

$$\frac{Lift}{Drag} = \frac{\langle F_y \rangle}{\langle F_z \rangle} = \frac{\omega L}{R} = \frac{2\pi v}{\lambda} \frac{L}{R} \qquad (12)$$

As noted before, the Lift/Drag ratio increases monotonically with velocity.

At this point it is useful to calculate the levitating efficiency, i.e., Newtons of levitating force per Watt of power dissipated in the track. This parameter is useful in evaluating proposed designs and is directly related to the Lift/Drag ratio. The average power, <P>, dissipated per circuit is given by the product $v\langle F_z \rangle$. Therefore, from equation 12),

$$\frac{\langle F_y \rangle}{\langle P \rangle} = \frac{2\pi}{\lambda} \frac{L}{R} \text{ Newtons/Watt} \qquad (13)$$

Comparing equation (13) for the power efficiency and equation (10) for the lifting force, we see that for any given circuit resistance, R, we can obtain any desired degree of efficiency by increasing the loading inductance, L, but necessarily at the expense of the reducing the lifting force per circuit.

The favorable effect of inductive loading on the efficiency comes about for two reasons: First, it shifts the phase of the current by 90°, corresponding to the optimum phase for producing lift by interaction with the z component of the magnetic field. Second, since the circuit power losses vary as the square of the current, while the lifting force only varies linearly with current, inductive loading (reduces the current) operates to increase the efficiency over what can be obtained for unloaded circuits, or, in the continuum limit, over that associated with eddy current losses in a sheet of conducting material. The gains that can be obtained practically will therefore be determined by a compromise between power efficiency (increases with inductive loading) and the lifting force per circuit (decreases with inductive loading).

Returning to equation (10) for the lifting force exerted by a single circuit, we must now consider the collective levitation force exerted by a close-packed array of circuits. We will assume, as noted earlier, that each circuit has a width in the z-direction of d_c m, that is, that there are $(1/d_c)$ circuits per meter. Thus total levitation force per meter will be given by summing the contribution from each circuit. It follows that the total levitating force exerted underneath a Halbach array that is one wavelength in length will be given by the expression:

$$\Sigma\langle F_y\rangle = \frac{\lambda B_0^2 w^2}{2kL}\frac{1}{1+(R/\omega L)^2}\exp(-2ky_1) \quad \text{Newtons/wavelength} \cdot (14)$$

Since the area of the Halbach array per wavelength in the z-direction is $w\lambda$ m^2, we find for the levitating force per unit area of the Halbach array the value:

$$\frac{\Sigma\langle F_y\rangle}{A} = \frac{B_0^2 w}{2kL}\frac{1}{1+(R/\omega L)^2}\exp(-2ky_1) \qquad \text{Newtons/m}^2 \qquad (15)$$

For the special case M = 4 (four magnet bars per wavelength), inserting the definition of B_0 (equation (6)), we find the result in terms of the remanent field, B_r :

$$\frac{\Sigma\langle F_y\rangle}{A} = \frac{4}{\pi^2}\frac{B_r^2 w}{kd_c L}\frac{1}{1+(R/\omega L)^2}[1-\exp(-kd)]^2\exp(-2ky_1) \qquad (16)$$

We consider now the quantitative constraints on the resistance, needed to evaluate real systems. In the embodiment of the circuits here being considered, the conductor array resembles rectangular window frames. We will take the length of the upper and lower legs of these rectangles to be equal to w m., i.e., the same as the transverse length of the magnets. Since $w >> \lambda$ can be assumed in most cases, we will take the length of the vertical legs of the circuit, h, to be equal to w/2. Thus the perimeter of the circuit, P_c, is taken to be 3w m:

$$P_c=3w$$

We further assume that the circuits form a close-packed array, made up of multiple turns of multi-stranded wire forming a bundle of rectangular cross-section. The width in the z direction, d_c m., of each bundle should be small compared to the wavelength, so that flux cancellation does not occur. Also, the depth of the bundle, Δ_c m, (in the y direction) must be small compared to the wavelength. Owing to the exponentially rapid fall-off of the magnetic field in this direction deeply located conductors would be ineffective in producing lift.

Considering the factors mentioned above we will take the circuit coils to be made of conductors the packing fraction of which is f (fractional area of conducting material). Typical values of f might be 0.8 to 0.9. We will also assume that there are β circuits per quarter-wavelength, i.e., their width in z, d_c, is $\lambda/4\beta$ m. Similarly, we will take the thickness of the circuit bundle in the y direction, Δ_c, to be equal to $\lambda/4\gamma$ m. That is, the bundle has a thickness in y which is a fraction $1/4\gamma$ of a wavelength. Given these parametric variations we may now define the single-turn-equivalent resistance of each circuit as being given by:

$$R=\rho\frac{Length}{Area}=\frac{16P_c\rho\beta\gamma}{f\lambda^2}=\frac{48w\rho\beta\gamma}{f\lambda^2}, \text{ ohms,} \qquad (17)$$

where ρ ohm-m. is the resistivity of the conductor (1.7×10^{-8} ohm-m. for copper, for example).

To continue the process of developing equations useful in arriving at practical designs, we will take as a design parameter the ratio of lifting force to power loss, as defined in equation (13). That

is, we define a parameter, K Newtons/Watt, through the relationship given in equation (13):

$$K = \frac{\langle F_y \rangle}{\langle P \rangle} = \frac{2\pi L}{\lambda R} \qquad \text{Newtons/Watt} \tag{18}$$

Note that as defined the K factor is closely related to the previously defined transition speed, that is, the speed where $\omega L/R \geq 1.0$. From this definition we see therefore that transition occurs when the condition $Kv \geq 1.0$ is satisfied, where v is in meters per second. K=2.0 therefore corresponds to a transition speed of 0.5 meters per second or 1.8 km/h (a slow walk!).

Using K as a design parameter allows us to eliminate the inductance from the equations for the lifting force. That is:

$$L = \frac{K\lambda R}{2\pi} \qquad \text{h y} \tag{19}$$

Inserting also now equation (17) for the resistance into equations (16) and (18), we are led to a design equation for the lifting force per square meter in terms of these parameters:

$$\frac{\Sigma\langle F_y \rangle}{A} = \frac{B_0^2 f \lambda}{24 K \rho \gamma} \frac{1}{1+(Kv)^{-2}} \exp(-2ky_1 - k\Delta_c), \qquad \text{Newtons/m}^2 \tag{20}$$

As will later be derived, the parameter K has a lower bound, set by the effect of mutual inductance between the windings. Thus the levitating force per unit area predicted by equation (20) has an upper bound. This bound in effect arises from the aforementioned constraint imposed by the magnitude of the Maxwell stress tensor associated with the magnetic field produced by the Halbach array. However, none of the Inductrack examples given herein will approach this upper bound.

B. An Example of an Inductrack System

An example, using parameters that might be appropriate for a levitated train car, will now be given to illustrate the potentialities of the Inductrack concept. We choose λ = 0.5 m., w = 1.0 m., B_0=0.9 Tesla (equation 6, with B_r=1.25 Tesla), and magnet thickness, d=λ/4), K = 2.0 N/Watt, f = 0.8, γ = 4 (1/16 of a wavelength circuit thickness

in the y direction), and $\rho = 1.7 \times 10^{-8}$ ohm-m. (copper). At v exceeding a few meters per second, we find from equation (20) a levitating force per square meter having the value:

$$\frac{\sum\langle F_y \rangle}{A} = 6.8 \cdot 10^4 \exp(-2ky_1)$$

The maximum force, occurring at $y_1=0$, corresponds to the levitation of about 7000 kilograms per square meter of magnet array, i.e., about 15 percent of the maximum limiting value (derived in Section V - equation 29). For the magnet array with its depth of $\lambda/4=0.125$ meters, the mass per square meter is about 900 kilograms, so that the maximum lifting force in this example corresponds to about 8 times the mass of the magnet array. At a K factor of 2.0 N/Watt, the power required to levitate 10,000 kilograms would be about 50 kW. To levitate a railroad car, such as the one considered in the study by Grumman [6], weighing 50,000 kilograms, would then require of order 7.0 square meters of magnet array (about 6 percent of the area of the undercarriage of the car), and would imply a drag load of about 250 kW, or about 3 percent of the 8.3 MW required to overcome aerodynamic drag at 500 km/h.

As previously mentioned, the approximate transition speed for a K value of 2.0 is about 1.8 km/h, a very low value compared to the operating speed. Also, at 500 km/h the Lift/Drag ratio, as calculated from equations (12) and (19), with K=2.0 and λ=0.5 m., is about 280.

Also, calculating backwards from the definition of K (equation 18) and the value of R for this example (calculated from equation 17), we find for the single-turn value of R the value 65 micro-ohms, and for L the single-turn value of 10.4 micro-henrys. Note that it does not matter electrically whether the circuit consists of a single turn occupying the entire cross-section, or of many turns having the same total cross-section: The L/R value for both cases will be the same. As a practical matter, for reasons cited earlier it will be preferable to use a circuit having many turns of multi-stranded wire, but the design calculations can be made as though the circuit is a single turn of wire of the given cross-section.

Now we evaluate the weight of copper per 1 m of the track. The thickness Δ_c of the winding is $\lambda/16=3.125 \cdot 10^{-2}$ m, its perimeter P_c in the xy-plane is 3 m, the filling factor f is 0.8, i.e., the volume of

copper per one meter is $f(\lambda/16)P_c=7.5\cdot10^{-2}$ m^3/m. Accordingly, the mass of copper is 0.67 t/m.

Knowing the mass of copper per unit length allows one to evaluate the temperature rise after a passage of a car through a certain point. The energy dissipated per unit length of a track is just <P>/v, where v is car velocity. In the aforementioned example, with <P>=250 kW and v=140 m/s, this energy is 1.8 kJ/m. As the thermal capacity of copper at room temperature is 0.385 kJ/kg^oK, the temperature rise is less than $10^{-2}K$ and therefore can be ignored.

As mentioned previously, there are obvious trade-offs that can be made in the design. For example, the adoption of a K parameter value of 1.0 (where this is allowed as a result of the choice of other parameters) would halve the magnet weight required at the expense of doubling the power required to levitate the car.

As will be discussed in a later section, the "window-frame" configuration of the Inductrack circuits here discussed is not necessarily the most efficient design or the one of least cost. The example given here should therefore only be considered as illustrative of the numbers involved. Note also that if in the example we had posited the use of the latest NdFeB magnet material, with a remanent field of 1.41 Tesla instead of the 1.25 Tesla value we assumed, and if we had taken M = 8 (number of magnet bars per wavelength), we would have obtained (using equation 6) a value of B_0 equal to 1.1 Tesla, corresponding to an increase of $(1.1/0.9)^2=1.5$ in the levitating power for the same magnet weight. This gain might be more than sufficient to compensate for the use of a (likely) more expensive magnet material, and a somewhat more complex magnet array.

In the loss calculations given up to this point the losses in the laminated iron inductive loading elements in the track have not been included. The reason for this omission is based on the fact that a preliminary estimate shows that when properly designed (using air gaps in the lamination stacks) the losses from these elements will be at most a few percent of the conductor losses. There will, however, again be an opportunity for optimization. That is, one might adopt designs with somewhat higher core losses in exchange for lower initial capital cost.

To summarize up to this point, using lumped-circuit approximations with some simplifying assumptions, equations have been derived that may be used for the design of one form of an Inductrack system. This system employs Halbach arrays interacting with a "track" consisting of a close-packed array of inductively loaded circuits the conductor bundles of which resemble window frames. That is, they are rectangular in shape and lie in vertical planes. The equations derived have been used to calculate the properties of an example system, one that would levitate a 50,000 kg car with the expenditure of 250 kW of drag power (3 percent of the aerodynamic drag at 500 km/h), employing magnet arrays that would comprise about 10 percent of the total weight of the car.

In the next section an analysis not involving the simplifying assumptions used in the lumped-circuit analysis will be outlined. In the proper limits this broader-based analysis corroborates the lumped-circuit results. Furthermore, it provides a means for correcting those results so as to include the effects of mutual inductance in the design equations in a simple way.

V) Effects of Distributed Inductance

Details of the corresponding analysis are presented in Appendices A1 through A4. Here we summarize main results and compare them with results of the previous section. In addition, we consider a modified version of the track design, in which the currents flowing on the upper surface of the track close, not through the lower leg of the circuit, but rather through highly conductive side walls.

A. Distributed Inductance in the Window-Frame Scheme

The current induced in any particular track conductor produces magnetic flux which couples with a number of neighboring conductors, occupying a length (in the z-direction) of order of $1/k$. The fact that the interaction occurs not just between two or three windings but rather between groups of them makes the analysis of the effect of mutual inductances somewhat complicated. However, as we show in the aforementioned appendices, the final result is remarkably simple: what should be changed in the basic equations (10), (11) of the previous section is simply to replace the self-inductance L of a winding by a sum $L+L^{(d)}$, with $L^{(d)}$ being a term responsible for the inductive interaction between the circuits (the superscript "d" stands for the word "distributed": we prefer to use

this term and not the term "mutual" because the former more fully reflects the essence of the effect). This contribution (of the dimension of inductance, Hy), has the form:

$$L^{(d)} = \frac{\mu_0 P_c}{2kd_c} \tag{21}$$

where P_c is the perimiter of a single track coil. Instead of our basic equation (15), we now have:

$$\frac{\sum\langle F_y\rangle}{A} = \frac{B_0^2 w}{2k\left(L+L^{(d)}\right)d_c} \cdot \frac{\exp(-2ky_1)}{1+\dfrac{R^2}{\omega^2\left(L+L^{(d)}\right)^2}} \tag{22}$$

while lift-to-drag ratio is now determined by the relationship

$$\frac{Lift}{Drag} = \frac{\omega\left(L+L^{(d)}\right)}{R} \tag{23}$$

Of course, in the limit $L^{(d)} << L$ one just recovers the results of Sec.IV. Note also that to take into account the finite thickness of the track one should replace y_1 in (22) by $y_1+(\Delta_c/2)$.

Using the above considerations, the example given in Section IV may be updated. To review, the parameters were: λ=0.5 m., B_0 = 0.9 Tesla (equation 6, with B_r=1.25 Tesla, and d=λ/4), K=2.0 N/Watt, f=0.8, γ=4 (1/16 of a wavelength circuit thickness in the y direction), and ρ=1.7 x 10^{-8} ohm-m. (copper).

We first establish whether the assumed value of K exceeds its lower bound which is obviously set by the distributed inductance term equation (21). Here all parameters are known except P_c, which we have earlier taken to be equal to 3.0 w m. If we now take w = 1.0 m. for our example, then we find $L^{(d)} = 4.8 \cdot 10^{-6}$ Hy. We previously found for R the value $65 \cdot 10^{-6}$ ohms. These numbers result in a K value of 0.92, approximately factor of 2 below our assumed value of 2.0.

An alternative means for the calculation of the minimum value of the design constant K is given in Appendix 9, equation (A9.5). It is there shown that this constant can be defined in terms of only three

parameters: the depth of the track conductors, Δ_c, the packing fraction of the windings, f, and the resistivity of the conductor material, ρ. In terms of these parameters we then have the result:

$$K_{min} = \frac{\mu_0 f \Delta_c}{2\rho} \qquad \text{Newtons/Watt}$$

Inserting the numbers for the above example, with $\Delta_c = \lambda/4\gamma = 0.03125$ m., we again find $K_{min} = 0.92$.

Returning to the question of the added inductance, it follows from equation (19) that at a K value of 2.0, with the given resistance the total inductance should be equal to $10.3 \cdot 10^{-6}$ Hy. Thus the added single-turn inductive loading should be $(10.3\text{-}4.8) = 5.5 \cdot 10^{-6}$ Hy.

The Lift/Drag ratio is unchanged from the value of 280 previously calculated, except that we now recognize the important role of mutual inductance in determining the effective inductance of the circuits.

All other numbers remain unchanged from those given previously.

It is convenient to present the lift-to-drag ratio in the form:

$$\frac{Lift}{Drag} = \frac{kvL^{(d)}}{R}\left(1+\frac{L}{L^{(d)}}\right) \equiv v\lambda\frac{\mu_0 f}{8\rho\gamma}\left(1+\frac{L}{L^{(d)}}\right) \qquad (24)$$

If the dimensionless geometrical factors (f, γ) and the ratio $L/L^{(d)}$ are kept constant from one design to another, then the lift-to-drag ratio scales as a product of the wavelength (λ) and car velocity (v). Therefore, for a small and slow system, one may have to introduce considerable lumped self-inductances, $L >> L^{(d)}$, in order to reach a high enough value of lift/drag. For large, fast systems the required self-inductances become comparable with or even smaller than $L^{(d)}$. Thus we conclude that relative role of lumped inductances increases with the transition to smaller and slower systems.

B. A "Flat" Track Design

The continuum approach can be used to analyze another configuration of the Inductrack, one possibly possessing economic and other advantages over the "window frame" configuration that has been analyzed in the preceding sections.

The geometry of the alternate configuration is shown schematically in Fig. 5. As can be seen, this configuration is made up of a close-packed array of conductors lying transversely in the surface of the track. However, instead of continuing the circuit below the surface of the track, as in the window-frame design, all conductors are terminated at each end by a low-resistance bus bar through which all return currents flow. To provide inductive loading, rings of ferromagnetic material are placed around the conductors near their ends (i.e., before the conductors connect with the bus bar).

To minimize the ohmic losses, every conductor should be made by a litz wire technique, with every particular current lead crossing the thickness of the track up and down several times (Fig. 6). This configuration will make the current distribution uniform over the thickness of the conductor. (If one makes conductor of a solid uniformly conducting rod, the current would be concentrated only within a skin-depth of the surface, thus increasing resistive losses). Each current lead, traversing between the upper and the lower surfaces, could be, again, composed of litz wire, thereby minimizing eddy current losses.

The potential gains that can be provided by this design, are four-fold: first, we reduce the ohmic losses compared to the window-frame design, simply because the length of a conductor becomes half as long as in this former design; second, because the mutual inductance term also decreases proportionally to the conductor length, one could increase the maximum lift force, as shown by equation (22); third, we reduce the weight of conductor, thereby reducing the cost of the track; fourth, the amount of ferromagnetic material used in the inductive loads can also be reduced. (To maintain the same L/R ratio, it should be reduced, roughly speaking, proportionally to the conductor length).

A disadvantage of this scheme is that one might have to use more expensive custom-made litz conductors, instead of using multiturn windings as in previous designs.

Engineering design equations for the "flat" design remain basically the same as for the "window-frame" design, with an obvious identification of the perimeter of the conductor P_c with the width of the conductor between bus-bars. As an illustration of possible parameters of this scheme, we repeat calculations of the Section IVB for the "flat" design, assuming that the width of the track between the bus-bars is

$$P_c=1.2\ w \tag{25}$$

Accordingly, instead of equation (17), we have

$$R=\frac{19.2\rho\beta\gamma w}{f\lambda^2}\ \ Ohms \tag{26}$$

As we show in Appendix 4, to take into account Ohmic losses in the bus bars, one should increase R by some "added resistivity"

$$R_{Add}=\frac{\rho}{kd_c\delta}\ \ Ohms \tag{27}$$

with δ being a skin-depth in the bus bar material,

$$\delta=\sqrt{\frac{2\rho}{\omega\mu_0}} \tag{28}$$

Other design parameters will be kept the same as before, i.e., w=1.0 m, λ = 0.5m, d= λ/4, K = 2.0 N/Watt, f= 0.8, γ = 4 (i.e., Δ_c= d/4 = λ/16), β=4 (i.e., d_c = d/4 = λ/16). Then, according to equation (26), the resistance of a single conductor is reduced by a factor of 2.5 (to 26 micro-ohms). The added resistance at the speed of 500 km/h is 12 micro-ohms. Therefore, the total resistance is 38 micro-ohms, approximately 1.7 times less than in a window-frame design. To keep the parameter K constant, one should reduce the total inductance by the same factor. Therefore, instead of a total inductance $L+L^{(d)}$ of 10.4 microhenrys, we should have a total inductance of 6.1 microhenrys. Of this total, according to equations (21) and (25), 1.92 microhenry would come from the effect of distributed inductances. Thus, the lumped self-inductance of each conductor should be 4.3 microhenrys.

As the total inductance is reduced by a factor of 1.7 compared to the example considered in Sec. IVB, the lift force increases by a factor of 1.7 (to approximately 11 t/m^2). The weight of conductor and ferritic material in the track is reduced by factors 2.5 and 1.3, respectively. As we kept parameter K constant, the lift-to-drag ratio remains unchanged (280 at the speed 500 km/h).

If one wants to push the lift force to its maximum possible level achievable with the "flat", track design, one has to reduce the length of the conductors to the minimum value $P_c=w$ and completely eliminate ferritic inductive elements (make L=0). Then, equation (22) in the limit of high speed ($\omega L^{(d)}/R>>1$) yields:

$$\frac{\sum\langle F_y^{\max}\rangle}{A}=\frac{B_0^2}{\mu_0}\exp(-2ky_1-k\Delta_c) \tag{29}$$

Here we have explicitly taken into account the correction caused by the finite thickness of the conductor. For the Halbach array considered in Sec.VI (M=4, $d=\lambda/4$, $B_r=1.25$ Tesla), and $y_1=0$ and $k\Delta_c=\pi/8$ ($\gamma=4$) this force is equal to 44 Ton/m^2 (!). Of course, one should remember that, by making L=0, one somewhat decreases the lift-to-drag ratio. Still, this example shows that the absolute value of the lift force will hardly be a serious limiting factor in the inductrack design.

We may compare the maximum force (29) and the levitating force (22), at speeds where the resistive term in the denominator of (22) is small (i.e., the speed is large compared to the transition speed). In this limit we have:

$$\frac{\sum\langle F_y\rangle}{\sum\langle F_y^{\max}\rangle}=\frac{w}{P_c}\frac{L^{(d)}}{L+L^{(d)}} \tag{30}$$

We see that increasing the lumped self-inductances, L, decreases the lift force while, at the same time, it increases the lift-to-drag ratio. This is in a full agreement with conclusions drawn in Sec.IV.

C. A Track in the Form of a Conducting Slab

To compare the Inductrack with earlier proposals, one can consider a track made just of a slab of a conducting material, i.e., one

without any windings at all (Fig. 7). This design is indeed very simple but now the currents flow only in a relatively thin skin-layer (not being forced to occupy the whole thickness of the slab by Litz winding or multiturn winding techniques of the previous sections), and one can expect increased Joule losses and reduced lift-to-drag ratio.

As is shown in the Appendix 3, in the case under consideration the expressions for the lift force and for the lift-to-drag ratio read:

$$\langle F_y \rangle = \langle F_y^{max} \rangle \frac{\left(\sqrt{1+\frac{k^4\delta^4}{4}} - \frac{k^2\delta^2}{2} \right)^{3/2}}{k\delta + \left(\sqrt{1+\frac{k^4\delta^4}{4}} + \frac{k^2\delta^2}{2} \right)^{3/2}} \tag{31}$$

$$\frac{\langle F_y \rangle}{\langle F_z \rangle} = \frac{1}{k\delta} \left(\sqrt{1+\frac{k^4\delta^4}{4}} - \frac{k^2\delta^2}{2} \right)^{1/2} \tag{32}$$

where F_y^{max} is determined by equation (29) and δ is a skin-depth within the conductor, given by equation (28).

The dependences given in equations (31) and (32) are illustrated in Figs. 8a and 8b for the case of a copper conductor (ρ=0.017 micro-Ohms m) and a wavelength of the Halbach array λ=0.5 m.

In the limit $k\delta << 1$ (skin depth small compared to the wavelength, as can expected to be the case in practical situations) the expression (32) reduces to:

$$\frac{\langle F_y \rangle}{\langle F_z \rangle} = \frac{1}{k\delta} = 2.425\sqrt{\lambda v} \qquad \text{for copper} \tag{33}$$

In this case, by contrast with the Inductrack scaling, above a critical speed (determined by the actual thickness of the sheet conductor as compared to the skin depth), although the Lift/Drag ratio also increases with the velocity, it varies only as the square root, rather than linearly. Furthermore, its numerical value at 500 km/h and at a wavelength of 0.5 m. has only risen to 20, more than an order of magnitude smaller than the L/D ratio in the example given in Section

IV. Although the magnetic field configuration of the Inductrack is not the same as used in earlier concepts, this example illustrates the substantial improvement in efficiency that is possible with the Inductrack concept, as compared to previous eddy-current-based systems.

VI) Brief Discussion of Some Practical Issues

Of course, evaluation of the Inductrack concept, as well as of any other new transportation concept, should be based not only on the "bare bones" design of the type presented in our report, but also on detailed discussion of a host of practical problems, ranging from resilience of the transportation system to possible attempts of vandalization, through possible effects of seasonal and diurnal temperature variations, of snow- and rain-falls, to limitations on the noises produced by the trains. For high-speed trains serious constraints can be imposed by the topography of the land. Many of the "practical" issues are more or less common for all high-speed systems, others are more specific. Here we will discuss only a few such issues which have direct relevance to the electrodynamical part of the concept as described in the present report.

The first issue is that of the gap between the track and the lower surface of magnet array. According to our master equation (22) this gap (y_1) strongly affects the lifting force. Theoretically, the gap can be made very small but in practical situations there exist important limitations on its minimum value. Indeed, if the car is a passenger car, then one must make provisions for its safe operation even if all passengers have moved to the front seats (or to the left seats) leaving the rest of the car empty. Let us, for instance, consider a scenario when all the passengers have moved to the front rows. This will cause a forward tilt of the car which will produce a restoring torque. Assuming that magnet arrays occupy only short sections of the car near the front and rear ends, one can easily find that the front end of the car will lower by the distance

$$\delta y_1 = \frac{m}{2k(m+M)} \tag{34}$$

where m and M are the masses of passengers and of the car, respectively (see first few paragraphs of Appendix 6 for relevant details). Clearly, the gap can not be made smaller than this distance.

Taking a factor 2 as the safety margin, we obtain the following limitation on the minimum possible gap width:

$$y_1 > \frac{m}{k(m+M)} \tag{35}$$

According to (22), for the mass of passengers equalling 20% of the mass of the car, this constraint means a 40% loss of the lifting force compared to its theoretical maximum (at $y_1=0$).

For the mass of passengers being 0.2 of the mass of the car, and for the wavelength λ=0.5 m, y_1 should exceed 1.33 cm; for the wavelength λ=1 m, y_1 should exceed 2.66 cm.

The other limitation of the gap is related to possible imperfections of the surface of the track, in particular, imperfections with a scale-length λ_{imp} in the z-direction of order of the car length L_{car}. The average gap should exceed with some margin the height of these non-uniformities.

Non-uniformities with long wave-length in z-direction (λ_{imp} much greater than L_{car}) can be of some concern if they would cause perturbations resonating with vertical oscillations of the car. The frequency Ω of the latter (see Appendix 6) is equal to $(2kg)^{1/2}$, i.e., for Halbach array with the wavelength of 0.5 m this frequency is equal to 16 s^{-1}. At the car speed of 140 m/s, these oscillations will resonate with the wavelength $\lambda_{imp} \approx 60$ m.

At very high car speeds the car will possibly experience an action of pulsating forces arising from the vortex air flow around the car. The distance between the car bottom and the track should be sufficient to accomodate the time-dependent tilts arising from these forces. Quantitative limitations will become clear after a preliminary aerodynamical design of the car has been made.

Added to the thickness of the gap should be also the thickness of a protection layer which should be placed on the upper surface of the track windings (between the windings themselves and the bottom of the car) and which should protect the windings from mechanical damage. This layer should be insulating (or have a low conductivity) to avoid eddy current losses in it. Its thickness should probably be about 0.5 cm. Taking into account all these

considerations, we assume that the gap y_1 can be made equal to 3.125 cm. Of course, there is a considerable degree of arbitrariness in this choice. One reason for choosing this particular number is that it corresponds to 1/16 of the wavelength λ=0.5 m and thereby considerably simplifies numerical estimates. This gap will also allow for a thin metallic sheath over the surface of the magnet array, to protect it from damage.

The electromotive force, V, induced by the periodically varying magnetic field in each conductor is equal to $d\phi/dt$. Its amplitude, according to equation (7) (with exp(-kh) neglected), is

$$V=wvB_0\exp(-ky_1)$$

Taking w=1 m, v=140 m/s and $B_0\exp(-ky_1)$=0.7 T, we find that the electromotive force is approximately 100 V. Most of this voltage drop occurs over the lumped inductances. However, the value of 100 V is easily manageable and should not cause concern.

The forces acting on conductors will have not only a vertical component acting downward but also a horizontal component of comparable amplitude and with a sign alternating at the wave period. According to our estimates of the lift force (see Sec.IVB) this horizontal component is of order of 10 t/m^2. The mechanical structure of the track should be made strong enough to withstand these tangential stresses.

VII) Summarizing Examples and Equations

In this section we present in a compact form self-consistent sets of parameters for several track and magnet designs (TABLES 1 and 2). In these designs we assume that the number of magnets per wavelength of the Halbach array is M=4, the remanent magnetic field is B_r=1.25 T, the width of the array is w=1 m, the thickness of the magnets is d=0.125 m, magnet material has a density of 7.2 t/m^3 (accordingly, the weight of the magnets is 0.9 t/m^2), the thickness of the conductor in the track is Δ_c=0.03125 m, the width of the conductor in z-direction is d_c=0.03125 m, the filling factor is f=0.8, the gap between the lower surface of the magnets and the surface of the conductors is y_1=0.03125 m, the Newton/Watt parameter is K=1 s/m for TABLE 1 and K= 2 s/m for TABLE 2. To find the power lost in the track (in MW), one should multiply the weight of the car in

tonnes by the factor 0.0098/K. For reference purpose, we note that, for the Grumman design of the magnetically levitating car weighing 50 tonnes, aerodynamic losses were calculated to be 8.3 MW. The calculated power required for levitation in this example is about 500 kW, or 6 percent of the propulsion power at 500 km/s.

The parametric variations of various quantities of interest, such as the Lift-to-Drag ratio and the levitation force vs speed, the variation of levitating force with levitation height, the power required for levitation, and the maximum levitated mass, are illustrated graphically in Figs. 9, 10, 11, 12, 13, and 14. Figs. 13 and 14 are comparisons, in block graph form, of the levitation power and the maximum levitated mass for three different cases: (1) a conducting surface (copper), (2) a flat track with no extra inductive loading, and, (3) an inductively loaded flat track with K = 3.0. All three cases are for a Halbach array wavelength of 1.0 m. The trade-offs between drag power and levitating force can be seen from these plots. Also obvious from the plots is the marked increase in efficiency associated with the Inductrack system, as compared to conventional eddy current-based systems.

Finally, we summarize the equations needed to calculate the above quantities in terms of the basic design parameters B_0, λ, ρ, γ, f, and K, the separation and winding thickness parameters, y_1 and Δ_c, respectively, and the velocity, v. The dimensionless parameter γ, is equal to the ratio of a quarter-wavelength to the winding thickness, Δ_c, (i.e., $\gamma = 4$ corresponds to the case $\Delta_c = 1/4(\lambda/4) = \lambda/16$), so that either one may be calculated in terms of the other one.

We have for the levitating force of the window-frame Inductrack , in Newtons/m^2 (Equation 20):

$$\frac{\Sigma\langle F_y\rangle}{A} = \frac{B_0^2 f\lambda}{24K\rho\gamma}\frac{1}{1+(Kv)^{-2}}\exp(-2ky_1 - k\Delta_c), \qquad \text{Newtons/m}^2$$

For the minimum value of the parameter K (no added inductive loading) we have (equation A9.5 of Appendix 9):

$$K_{min} = \frac{\mu_0 f\Delta_c}{2\rho} \qquad \text{Newtons/Watt}$$

For the Lift-to-Drag Ratio we then have, for the window-frame Inductrack:

$$\frac{Lift}{Drag} = \frac{kvL^{(d)}}{R}\left(1+\frac{L}{L^{(d)}}\right) \equiv v\lambda\frac{\mu_0 f}{8\rho\gamma}\left(1+\frac{L}{L^{(d)}}\right)$$

The first part of this equation is general, and can be used to calculate the Lift-to-Drag ratio for the flat-track, inserting the value of R and the distributed inductance, $L^{(d)}$, appropriate to that geometry.

For the flat-track design with a circuit perimeter equal to 1.2w, (w is the width of the track facing the Halbach array), the value of R is given by the expression (equation 26):

$$R = \frac{19.2\rho\beta\gamma w}{f\lambda^2} \quad Ohms$$

For the distributed inductance, $L^{(d)}$, we have (equation 21):

$$L^{(d)} = \frac{\mu_0 P_c}{2kd_c} \quad \text{hy}$$

where P_c is the perimeter of either the window-frame coil or the flat-track coil.

For the flat-track Inductrack we have for the maximum value of the levitating force (occurring when the width of the track, w, facing the Halbach array is equal to P_c) the expression (equation 29):

$$\frac{\sum\langle F_y^{max}\rangle}{A} = \frac{B_0^2}{\mu_0}\exp(-2ky_1 - k\Delta_c) \qquad \text{Newtons/m}^2$$

For both the window-frame and the flat-track systems we have for the ratio of the lifting force to its maximum possible value the expression (equation 30):

$$\frac{\sum\langle F_y\rangle}{\sum\langle F_y^{max}\rangle} = \frac{w}{P_c}\frac{L^{(d)}}{L+L^{(d)}}$$

Finally, we have for the maximized ratio of the levitated weight to the magnet weight, the expression (equation A7.5 of Appendix 7):

$$\left[\frac{\text{Wt. lev.}}{\text{Wt. mag.}}\right]_{\max(kd)} = 26.31 \left[\frac{B_r^2}{\lambda}\right](\exp[-2k(y_1-\Delta_c/2)]$$

VIII) Concluding Remarks

The analyses presented in this report show that the Inductrack concept represents a viable approach to the passive magnetic levitation of moving objects. As has been described, it operates by exploiting the repelling force between magnets on the moving object interacting with currents induced in a stationary track. However, the Inductrack concept is to be distinguished from earlier induced-current passive magnetic systems by the fact that its configurations, involving close-packed conductor arrays and optimally efficient arrays of permanent magnets, lead to markedly improved characteristics relative to those earlier approaches. Specifically, the levitating forces can be made to approach the theoretical maximum value achievable by the levitating magnetic fields, i.e., that value associated with movement of the magnet array over a perfectly conducting surface. In addition, the Lift-to-Drag ratios, increasing linearly with speed, can reach values in excess of 200, one to two orders of magnitude higher than those typical of earlier systems. Correspondingly, the "transition speeds", i.e., those speeds at which magnetic levitation begins to become effective, are much lower than those for other systems, being as low as one or two kilometers per hour. An important additional feature is that by taking advantage of the special magnet array design (Halbach arrays), and of new high-field permanent magnet materials, it is not necessary to contemplate the use of electromagnets employing superconducting coils in order to achieve adequate levitation forces relative to the weight of the levitating magnets. With the Inductrack system the ratio of levitated weight to magnet weight can, in typical cases, be in the range of 10:1 to 40:1. The higher of these values is an order of magnitude greater than values that have been quoted for some earlier systems.

For the designer of magnetically levitated systems, one important consequence of our analyses is that the results can be reduced to simple yet accurate design formulae, allowing for

characterization and optimization prior to actual construction. To be discussed in another report is the analysis of the general stability of the system. Here again the simplicity of the Inductrack concept and its tractability for analysis leads to well-defined criteria for passively stable operation. With the Inductrack there is no requirement for active stabilizing control circuitry of the type required for some other approaches to the magnetic levitation, those that must deal with the intrinsic instability of magnetic levitation implied by Earnshaw's theorem.

Although this report has not dealt, other than superficially, with the topic of costs and economics, it seems probable that the basic simplicity of the Inductrack concept should translate to economic practicality in high-speed transit systems, particularly when the "fail safe" nature of the concept is taken into account.

Work performed under the auspices of the U.S. Department of Energy by the Lawrence Livermore National Laboratory under Contract W-7405-Eng-48.

Appendix 1.
Fourier Decomposition of the Magnetization Currents and of the Magnetic Field of a Halbach Array

We consider a Halbach array of the form shown in Fig.3, i.e., with four magnet bars per wavelength. It is assumed that this system is continued periodically in both directions of axis z. Direction of magnetization of each particular bar is shown by arrows. The absolute value of remanent magnetic field is identical for all the rods and is equal to B_r. The linear density of the magnetization current that flows on the boundaries between the bars is:

$$I=B_r/\mu_0 \qquad \text{(A1.1)}$$

where μ_0 is permeability of free-space ($4\pi\cdot 10^{-7}$ $H\cdot m^{-1}$). Directions of the magnetization currents are shown by dots (to the observer) and crosses (from the observer). The current density corresponding to this current pattern can be written on the interval $0<z<\lambda/2$ as follows:

$$j_x(y,z)=I\{[\Sigma(y-y_1-d)-\Sigma(y-y_1)]\cdot[\delta(z-\lambda/8)+\delta(z-3\lambda/8)]+ [\Sigma(z-3\lambda/8)-\Sigma(z-\lambda/8)]\cdot[\delta(y-y_1)-\delta(y-y_1-d)] \qquad \text{(A1.2)}$$

where Σ is a Heavyside step-function (equal to 1 at positive values of its argument and to zero at the negative values). At $-\lambda/2<z<0$ the current density can be found from the condition $j_x(y,-z)=-j_x(y,z)$. Outside the interval $-\lambda/2<z<\lambda/2$ the current density can be found by periodic continuation.

As $j_x(x,z)$ is an odd function of z, its Fourier decomposition in z will contain only sines (no cosines):

$$j_x(y,z)=\sum_n j_n(y)\sin(2n\pi/\lambda)z \qquad \text{(A1.3)}$$

where

$$j_n(x)=\frac{2}{\lambda}\int_{-\lambda/2}^{\lambda/2} j_x(y,z)\sin nkz\,dz = (8I/\lambda)\sin(n\pi/2)\{[\Sigma(y-y_1-d)-\Sigma(y-y_1)]\cdot$$
$$\cdot\cos(n\pi/4)+(1/kn)\cdot[\delta(y-y_1)-\delta(y-y_1-d)]\sin(n\pi/4)\}, \qquad \text{(A1.4)}$$

with

$$k=2\pi/\lambda \qquad \text{(A1.5)}$$

being a wave-number of Halbach array. Obviously, the Fourier coefficients are non-zero only for odd n's (n=1, 3, etc).

It is instructive to find the magnetic field produced by separate Fourier-harmonics of the current. We present expressions for magnetic field below ($y<y_1$) and above ($y>y_1+d$) the magnet array:

$$B_{zn}=-\frac{2\mu_0 I}{\pi n}\sin\frac{n\pi}{2}\cdot(\cos\frac{n\pi}{4}+\sin\frac{n\pi}{4})\cdot e^{kn(y-y_1)}\cdot(1-e^{-nkd})\cdot\sin knz \quad \text{(below)}$$
$$B_{zn}=-\frac{2\mu_0 I}{\pi n}\sin\frac{n\pi}{2}\cdot(\cos\frac{n\pi}{4}-\sin\frac{n\pi}{4})\cdot e^{kn(y-y_1-d)}\cdot(1-e^{-nkd})\cdot\sin knz \quad \text{(above)} \qquad \text{(A1.6)}$$

Note that only Fourier harmonics with n=1, 5, 9, etc contribute to the magnetic field below the array and, only harmonics with n=3, 7, 11, etc contribute to the magnetic field above the array. As amplitudes of the harmonics are inversely proportional to n, this means that magnetic field is much stronger on the lower side of the magnet than it is on the upper side. This circumastance is one of attractive features of the Halbach array: The magnetic field is concentrated just on that side of the array where it (the magnetic field) interacts with the track and provides lifting force.

For n=1, the magnetic field determined from (A1.6) coincides with the expression (4) of the main text.

On the lower side of the array, the first harmonic of the magnetic field is strongly dominant: the next non-vanishing harmonic is n=5. The amplitude of this harmonic is 5 times less than of the main one. Magnetic forces are proportional to the square of the magnetic field. If we average them over the wavelength λ, the interference between different harmonics disappears because of their orthogonality. Therefore, the 5th harmonic gives only, roughly speaking, a 4% contribution to the forces. This allows us to neglect effects of all the harmonics but the first one in evaluating the forces acting on the Halbach array from the side of the track.

Appendix 2
Evaluation of Distributed Inductance

In this Appendix we consider a Halbach array moving parallel to the track surface in the direction z. For the system whose length in x direction is large compared to λ, the magnetic field can be uniquely described by the x-component of the vector-potential $A_X \equiv A(y,z)$:

$$B_y=\partial A/\partial z;\ B_z=-\partial A/\partial y \qquad \text{(A2.1))}$$

The vector-potential satisfies Poisson equation:

$$\nabla^2 A = -\mu_0 j_x(y,z) \qquad \text{(A2.2)}$$

where j_X comprises both magnetization current and the conductivity current in the slab. As has already been mentioned, it is accurate enough to retain only the first Fourier harmonic n=1 of the magnetization current (A1.3), i.e., to represent a magnetization current density in the form:

$$j_x^{(m)} = \frac{4\sqrt{2}I}{\lambda}\left\{\left[\Sigma(y-y_1-d)-\Sigma(y-y_1)\right]+\frac{1}{k}\left[\delta(y-y_1)+\delta(y-y_1-d)\right]\right\}\sin\left[k(z-vt)\right] \equiv$$

$$\tilde{j}^{(m)}(y)e^{i(kz-\omega t)}+c.c. \qquad \text{(A2.3)}$$

where the subscript "m" designates magnetization current, and

$$\tilde{j}^{(m)}(y)=\frac{2\sqrt{2}I}{i\lambda}\left\{\left[\Sigma(y-y_1-d)-\Sigma(y-y_1)\right]+\frac{1}{k}\left[\delta(y-y_1)+\delta(y-y_1-d)\right]\right\} \qquad \text{(A2.4)}$$

$$\omega=kv \qquad \text{(A2.5)}$$

The solution of equation (A2.2) for A should have the same form as equation (A2.3), i.e., A should be represented as:

$$A=\tilde{A}(y)e^{i(kz-\omega t)}+c.c. \qquad \text{(A2.6)}$$

The equation for $\tilde{A}$ reads:

$$\frac{d^2\tilde{A}}{dx^2}-k^2\tilde{A}=-\frac{4\pi}{c}\tilde{j} \qquad \text{(A2.7)}$$

We first consider the solution of equation (A2.7) in the upper half-plane (y>0). The solution can be represented as a sum of two terms: the vector potential $\tilde{A}^{(m)}$ produced by the magnetization current, and the vector potential $\tilde{A}^{(c)}$produced by the conductivity current in the track. The former can be easily found from equations (A2.1) and (A1.6). We will need an expression for $\tilde{A}^{(m)}$ only *below* the Halbach array. In this domain

$$\tilde{A}^{(m)}=-\frac{B_r\sqrt{2}}{\pi k}e^{k(y-y_1)}\left(1-e^{-kd}\right) \qquad \text{(A2.8)}$$

To find $\tilde{A}^{(c)}$, we must first to know the current in the track. But the functional dependence of $\tilde{A}^{(c)}$ on y is clear (as $\tilde{A}^{(c)}$ satisfies equation (A2.7) with r.h.s. equal to zero - no conductivity currents above the track):

$$\tilde{A}^{(c)}=C\exp[-k(y-y_1)] \qquad \text{(A2.9)}$$

where C is some constant (which, indeed, is determined by the current in the track).

The force acting on the Halbach array is determined by the interaction of the magnetization current and that part of the magnetic field which is produced by the currents in the track. In other words, the lifting force F_y (per unit area) is equal to:

$$F_y=\int\left\langle j_x^{(m)}B_z^{(c)}\right\rangle dx \qquad \text{(A2.10)}$$

The angular brackets denote averaging over the wavelength. Using the presentation in equation (A1.3) for $j_y^{(m)}$, one obtains:

$$F_y = -k\int\left(\tilde{j}_x^{(m)}C + c.c.\right)e^{-ky}dy = \frac{8\sqrt{2}I}{\lambda}e^{-ky_1}\left(1-e^{-kd}\right)\mathrm{Im}\,C \qquad \text{(A2.11)}$$

In the same fashion, one obtains the drag force F_Z:

$$F_z = -\int\left\langle j_x^{(m)}B_y^{(c)}\right\rangle dy = \frac{8\sqrt{2}I}{\lambda}e^{-ky_1}\left(1-e^{-kd}\right)\mathrm{Re}\,C \qquad \text{(A2.12)}$$

The parameter I in these equations is defined according to equation (A1.1).

Neglecting the thickness of the track compared to the other dimensions of the problem, we can approximate the current distribution in the track by a surface current, with a linear (per unit length in z) current density

$$I^{(s)} = \tilde{I}^{(s)}\exp(-i\omega t + kz) + c.c \qquad \text{(A2.13)}$$

From the condition that the jump of the tangential (z) component of magnetic field should be equal to $\mu_o I^{(s)}$, while the normal (y) component of the magnetic field should be continuous, we easily find C in terms of $\tilde{I}^{(s)}$:

$$C = \frac{\mu_0\tilde{I}^{(s)}}{2k} \qquad \text{(A2.14)}$$

Now we can find the magnetic flux under the track (it is this flux that induces the loop voltage that drives the conductivity current). Its temporal and spatial dependence is the same as equation (A2.13):

$$\phi = \tilde{\phi}\exp(-i\omega t + ikz) + c.c. \qquad \text{(A2.15)}$$

The contribution to this flux comes from the magnet array and the currents in the track:

$$\tilde{\phi} = -i\frac{B_r w\sqrt{2}}{\pi k}e^{-ky_1}(1-e^{-kd}) + \frac{\mu_0\tilde{I}^{(s)}P_c}{2k} \qquad \text{(A2.16)}$$

The current per conductor is equal to $I^{(s)}d_C$, and the contribution to the loop voltage from the lumped inductance is $-Ld_C(dI^{(s)}/dt)$. The total loop voltage V_{loop} has a form identical to equations (A2.13) or (A2.14), with

$$\tilde{V}_{loop} = i\omega(\tilde{\phi} + Ld_c\tilde{I}^{(s)}) \qquad \text{(A2.17)}$$

The loop voltage drives a current against the resistance of the conductor:

$$\tilde{V}_{loop} = R\tilde{I}^{(s)}d_c \qquad \text{(A2.18)}$$

Equations (A2.16)-(A2.18) allow one to find $\tilde{I}^{(s)}$ and, via relationships (A2.14) and (A2.11), the lift and drag forces. The results have been presented in the main body of our report (equations.(22) and (23)).

Our discussion pertained so far to the "flat" track design. It turns out that our main results remain valid also in the window-frame design, as long as the vertical dimension, h, of the frame remains large compared to 1/k. The cross-section should not even be necessarily rectangular, simply all the dimensions should be greater than 1/k. Indeed, in this case one can (conceptually) split the whole conductor into a number of (almost) straight segments of the length $\Delta l >> 1/k$; the contribution to Eq.(A2.16) from each segment will be $(\mu_0\tilde{I}^{(s)}/2k)\Delta l$, so that the contribution of the whole conductor will be just as given by Eq.(A2.16), with P_C having the meaning of a total perimeter of the conductor.

The other comment that should be made here is that we have neglected the presence of the high-permeability rings encircling every conductor. The corresponding corrections contain a small parameter equal to the ratio of the characteristic dimension of the ring and the perimeter P_C of the conductor.

Appendix 3
Magnetic Levitation Over a Conducting Slab

In this Appendix, we consider the electrodynamics of a Halbach array moving over the slab of a conducting material. We will assume that the slab thickness (Δ_c) considerably exceeds the skin-depth, so that one could replace the slab by a conducting half-space.

The contribution of the conductivity currents to the vector potential above the track is still determined by equation (A2.9). Therefore, the problem of finding lift and drag forces is again reduced to finding of the complex constant C. To do that, we first note that the vector potential inside the slab satisfies the usual skin-effect equation [7]

$$\frac{d^2\tilde{A}}{dy^2} - (k^2 + \frac{i\mu_0\omega}{\rho})\tilde{A} = 0 \qquad \text{(A3.1)}$$

The solution of this equation, one which exponentially decreases at negative y is:

$$\tilde{A} = D\exp(qy) \qquad \text{(A3.2)}$$

with

$$q = \sqrt{k^2 + \frac{i\mu_0 k\nu}{\rho}} \equiv \sqrt{k^2 + \frac{2i}{\delta^2}} \qquad \text{(A3.3)}$$

and δ being a standard skin-depth as defined by equation (28).

Above the conducting surface (but below the Halbach array) the vector potential is a linear superposition of equations (A2.8) and (A2.9),

$$\tilde{A}^{(m)} = -\frac{B_r\sqrt{2}}{\pi k} e^{k(y-y_1)}\left(1 - e^{-kd}\right) + C\exp - k(y - y_1) \qquad \text{(A3.4)}$$

From the condition that both $\tilde{A}$ and $d\tilde{A}/dx$ should be continuous on the y=0 surface, one finds that

$$C = i\frac{k-q}{k+q}\frac{\mu_0 I\sqrt{2}}{\pi k} e^{-ky_1}(1 - e^{-kd}) \qquad \text{(A3.5)}$$

Using equations (A2.11) and (A2.12) and separating the real and imaginary parts of C, one obtains after some algebra expressions (31) and (32) of the main text of the report.

Appendix 4
Resistive Losses in the Bus Bars

Consider magnetic fields and currents in the vicinity of the terminating bus bar, Fig.15. On this figure we do not depict lumped

inductances and do not show small up and down displacements of the neighboring conductors required to accomodate these inductive elements. Under conditions of practical interest, the skin-depth, δ, in the bus bar is smaller than 1/k, so that the current in the bus bar, in terms of its influence on the magnetic field outside the conductor, can be considered as a surface current. Qualitatively, the pattern of this surface current is shown by arrows on Fig.16.

The linear density of the surface current can be determined from conditions

$$I_y = \frac{B_z}{\mu_0};\quad I_z = -\frac{B_y}{\mu_0},\ \text{a/m} \qquad \text{(A4.1)}$$

where $\boldsymbol{B}$ is a magnetic field on the surface of the conductor. We consider a situation when the gap (in x-direction) between the Halbach array and the bus bars is greater than 1/k. Then the magnetic field on the bus-bar surface is entirely determined by expressions (A2.1), (A2.9), with only a contribution from the currents in the track playing a role.

The magnetic field of the track currents exponentially decays in the vertical direction, as also do the surface currents. In order not to increase resistivity, it is desirable to have the height of the bus bar larger than 1/k. We assume that this condition is satisfied.

As we can neglect the contribution of the Halbach array to the magnetic field on the surface of the bus bar, the problem becomes symmetric with respect to the surface of the track. We will consider only the region above the track. At y>0, the magnetic field can be presented as

$$\begin{aligned} B_y &= \tilde{B}_y \exp(-i\omega t + ikz - ky) + c.c. \\ B_z &= \tilde{B}_z \exp(-i\omega t + ikz - ky) + c.c. \end{aligned} \qquad \text{(A4.2)}$$

where $\tilde{B}_y$, $\tilde{B}_z$, are some constants related to each other through condition $\nabla \cdot \boldsymbol{B} = 0$:

$$\tilde{B}_y = i\tilde{B}_z \qquad \text{(A4.3)}$$

In case kd<<1, current inside the skin-layer varies proportionally to exp(-qx), with q=(1+i)/δ, and δ being the standard skin-depth, equation (31). Using this observation and relationships

(A4.1)-(A4.2), one can write the following expression for the current distribution in the bus-bar:

$$j_y = \frac{\tilde{B}_z q}{\mu_0}\exp(-i\omega t + ikz - ky - qx) + c.c.$$
$$j_z = -\frac{\tilde{B}_y q}{\mu_0}\exp(-i\omega t + ikz - ky - qx) + c.c. \qquad \text{(A4.4)}$$

The average power dissipated in the bus bars per unit length of the track (in z-direction) is:

$$Q_{BB} = 4\rho\int_0^\infty dx\int_0^\infty dy\left\langle j_y^2 + j_z^2\right\rangle \qquad \text{(A4.5)}$$

where ρ is the resistivity of the track, and the factor "4" in front of the integral takes into account the presence of two bus bars and the symmetry of the problem with respect to the horizontal plane. Simple integrations taking into account relationship (A4.3) yield:

$$P_{BB} = \frac{4\rho|q|^2}{k\,\mathrm{Re}\,q}\frac{\left|\tilde{B}_z\right|^2}{\mu_0^2} = \frac{8\rho}{k\delta}\frac{\left|\tilde{B}_z\right|^2}{\mu_0^2} \qquad \text{(A4.6)}$$

To express these losses in terms of resistive losses in the conductors, we first represent the surface current in the track in the form:

$$I_x = \tilde{I}_x\exp(-i\omega t + ikz) + c.c. \qquad \text{(A4.7)}$$

and then note that

$$\tilde{I}_x = \frac{2\tilde{B}_z}{\mu_0} \qquad \text{(A4.8)}$$

Resistive losses in the conductors per unit length of the track (in z-direction) are:

$$P_{Cond} = Rd_c\left\langle I^2\right\rangle = 2Rd_c\left|\tilde{I}\right|^2 = 8Rd_c\frac{\left|\tilde{B}_z\right|^2}{\mu_0^2} \qquad \text{(A4.9)}$$

where R is a resistance of a single (multiwire) conductor. From comparison of equations (A4.6) and (A4.9) one sees that the effect of the Ohmic losses in the bus bars can be described by adding some

resistance to the resistance of every conductor. This "added resistance" is

$$R_{Add} = \frac{\rho}{kd_c\delta} \qquad \text{(A4.10)}$$

Appendix 5
Eddy Current Losses in the Track

To be specific, we consider the geometry of the flat track. We evaluate the dissipation associated with eddy currents which are present in every separate wire of the conductor. The dissipation of these currents becomes particulary important when the "net" current which flows from one end of the conductor to another, is strongly suppressed, for instance, by large lumped inductances at the ends. In agreement with reality, we assume that the wire radius a is much less than the skin-depth (28), so that the wire is penetrated by the magnetic flux. This flux induces a vortex electric field which generates eddy currents, Fig.17.

We first find the eddy current dissipation in a single wire (many of such wires constitute the conductor) in a specific case when magnetic field intersecting the wire does not vary along its length. If the magnetic field, in fact, varies along the wire, then our results could be generalized by the introduction of a simple integration along the wire length.

The eddy current pattern in the wire is illustrated by Fig. 17 The direction of these currents is parallel to the wire axis everywhere except short ($\cong$ a) regions near the ends where these currents get closed across the wire. If we are not considering the vicinity of the ends, which gives only a small contribution to the dissipation (because the corresponding volume is small), then, using Faraday's law, we can write the following expression for the eddy current:

$$j_x = \frac{y\dot{B}_z - z\dot{B}_y}{\rho} \qquad \text{(A5.1)}$$

The power dissipated in the wire of the length w is

$$P = w\rho\int dydz\left\langle j_x^2\right\rangle, \text{ per wire} \qquad \text{(A5.2)}$$

where the integration is carried out over the wire cross-section and the angular bracket denotes averaging over the wave period. Elementary calculations yield:

$$P = \frac{\pi a^4 w \omega^2}{4\rho}\left(\left\langle B_y^2\right\rangle + \left\langle B_z^2\right\rangle\right), \text{ per wire} \qquad \text{(A5.3)}$$

Equation (A5.3) solves the problem of eddy current losses *in principle*. To make more concrete estimates, one has to have information regarding the magnetic field strength in the location of a particular wire. We will make these further calculations for the case when the lump inductances keep the total current in the conductor well below its maximum possible value determined by mutual inductances. This assumption corresponds reasonably well to the set of parameters for a "flat" track design considered in Sec.VB (L=4.3 microhenrys, $L^{(d)}$=1.9 microhenrys). In this situation, the magnetic field created by the currents in the track is small compared to the magnetic field created by permanent magnets and all the wires are exposed to the same magnetic field as determined by expressions (4), (5). In this case Eq.(A5.3) yields:

$$P = \frac{\pi a^4 w \omega^2}{4\rho} B_0^2 \exp(-2ky_1), \qquad \text{per wire} \qquad \text{(A5.4)}$$

The number of wires per conductor is, obviously, $d_c \Delta_c f / \pi a^2$. Therefore, the power dissipated per conductor is

$$P = \frac{a^2 w P_c \omega^2}{4R} B_0^2 \exp(-2ky_1), \text{ per conductor} \qquad \text{(A5.5)}$$

where $R = P_c / (f d_c \Delta_c \rho)$ is the resistance of the conductor bundle.

Now we will compare this result with the drag power per conductor. In case $L >> L^{(d)}$ which we are considering now,

$$P_{drag} = \frac{\left\langle F_y \right\rangle}{KA} w d_c = \frac{B_0^2}{K\mu_0} \exp(-2ky_1) \frac{w}{P_c} \frac{L^{(m)}}{L} w d_c =$$

$$= \frac{B_o^2}{K} \exp(-2ky_1) \frac{w^2}{2kL}, \qquad \text{per conductor} \qquad \text{(A5.6)}$$

(See relationships (18), (21), (29), (30); in the latter we neglect mutual inductance term in denominator). Dividing equation (A5.5) by

equation (A5.6), we find a convenient expression for eddy current dissipation *vs* main current dissipation:

$$\frac{\textit{Eddy current dissipation}}{\textit{Main current dissipation}} = \frac{K^2}{2}\frac{a^2\omega^2 P_c}{w} = (Kv)^2(ka)^2\frac{P_c}{2w} \qquad \text{(A5.7)}$$

For the design parameters discussed in Sec.VB (K=2 s/m, v=500 km/h=140 m/s, P_c/w=1.2, k=12.6 m^{-1}) this ratio is less than 1 for wires whose radius is less than, roughly speaking, 0.3 millimiters. The number of wires per conductor in the reference design is then approximately 2,000.

For thicker wires, eddy currents give a dominant contribution to dissipation. This, however, may be tolerable because the losses are still small: we can raise the losses in the track to, say, 30% of the aerodynamic losses and still remain in the domain of practical interest. Wires with radius of 1 millimeters (2 mm in diameter) would become then acceptable. Note that the power dissipation via eddy currents scales as v^2 (see (A5.5)) and at somewhat lower velocities (say, 150 km/h = 43 m/s) becomes quite modest. Also, if it is economically practical to use strands smaller than 0.3 mm in the litz wire, eddy current losses can always be made negligible compared to the resistive losses of the main current.

At high velocities (of order 500 km/h) the ω^2 dependence of the eddy current losses argues for increasing the wavelength of the Halbach array up to a limit determined by other economic factors. When the maximum advantage of this scaling has been taken and the smallest possible strand diameter has been used, the Inductrack concept can be evaluated versus the use of a uniform conducting slab, where eddy current losses are confined to the surface of the conductor. In some special circumstances the efficiency gains from using the Inductrack system might not be worth the extra complexity. One should note, however, that the unstructured track is incompatible with the concept of driving the car by controlled currents.

One caveat regarding the validity of equation (A5.5): When deriving it, we assumed that all the wires experience action of the same magnetic field. This may become incorrect in case of small (or non-existent) lumped inductances. In such cases the magnetic field may vary considerably between the upper and the lower sides of the

conductor (normal to the track). This effect can also be taken into account by performing integrations over the thickness of the conductor. We will, however, not present here these tedious derivations.

Appendix 6
Negative Damping of the Vertical Oscillations of the Car

In all other parts of this report we were considering steady-state motion of the car over the track. In this Appendix which somewhat deviates from the general course of this report, we consider damping of the vertical oscillations of the car. Much more detailed analyses of the car dynamics will be presented in a separate report [8]. However, evaluation of the damping rate is so tightly interwoven with the contents of the present report that we feel it appropriate to present this particular piece of mechanical analysis here. To be specific, we consider vertical oscillations of a car moving with a constant velocity. Somewhat surprisingly, the damping of vertical oscillations turns out to be negative. In other words, dissipative processes in the track tend to make these oscillations unstable. The energy that drives these oscillations comes from the work exerted on the car by the force that keeps it moving along the track with a constant speed.

Before evaluating the damping rate, we present a remarkably simple expression for the eigenfrequency of the vertical oscillations. For this we note that the lift force depends on the gap (y_1) between the magnets and the track in a universal way (see (22)):

$$F_y = const \cdot \exp(-2ky_1) \tag{A6.1}$$

where $const$ does not depend on y_1.

In the equilibrium state, the lifting force is equal to the weight of the car, Mg, where M is the mass of the car and g is gravity acceleration. We denote the equilibrium value of y_1 by $\bar{y}_1$ and consider small deviation δy with respect to it :

$$y_1 = \bar{y}_1 + \delta y \tag{A6.2}$$

Linearizing the lifting force with respect to δy, we immediately find that

$$\delta F_y = const \cdot \exp(-2k\bar{y}_1) \cdot (-2k\delta y) = -2Mgk\delta y. \qquad \text{(A6.3)}$$

Inserting this perturbation into Newton equation

$$M\delta\ddot{y} = \delta F_y, \qquad \text{(A6.4)}$$

we find the eigenfrequency Ω_0 of vertical oscillations:

$$\Omega_0 = \sqrt{2kg} \qquad \text{(A6.5)}$$

Remarkably, the only design parameter that enters this equation is the wavelength of Halbach array. For k=12,6 m^{-1} (λ=0.5m), this frequency is approximately 16 s^{-1} ($f_0 \approx 2.5$ Hz).

To proceed with evaluation of the damping coefficient, we return to equation (1) which we rewrite in the form:

$$L\frac{dI}{dt} + RI = -\frac{d\phi}{dt} \qquad \text{(A6.6)}$$

According to our previous results, by L here one should understand the total inductance per conductor (self+mutual) and by R a total resistance (self+added; the latter appears only for the "flat" track design). The flux term entering the r.h.s. of this equation is (Cf equation (7)):

$$\phi = (B_0 w/k)\exp(-k\bar{y}_1 - k\delta y)\sin k(z - vt) \approx (B_0 w/k)\exp(-k\bar{y}_1)(1 - k\delta y)\sin k(z - vt) \qquad \text{(A6.7)}$$

Our further plan is as follows: We consider a harmonic perturbation of y_1,

$$\delta y = \delta y_0 \cos(\Omega t) \qquad \text{(A6.8)}$$

and find an expression for the vertical force in this case. In this expression, in addition to the terms varying as $\cos\Omega t$, we find terms varying as $\sin\Omega t$. Being phase-shifted by 90° with respect to displacement, these terms are obviously responsible for the dissipation of vertical oscillations. From their amplitude, the damping rate of vertical oscillations can be easily found. This

approach is good as long as the damping rate of the oscillations is small compared with their frequency (and we will make this assumption).

Magnetic flux (A6.7) for y_1 as in (A6.2), (A6.8) can be presented as:

$$\phi = \phi_0\left\{\sin(kz-\omega t)-\frac{1}{2}k\delta y_0[\sin(kz-\omega_+ t)+\sin(kz-\omega_- t)]\right\} \qquad \text{(A6.9)}$$

where

$$\phi_0 = (B_0 w/k)\exp(-k\bar{y}_1),\ \omega = k\mathrm{v},\ \omega_+ = \omega+\Omega,\ \omega_- = \omega-\Omega \qquad \text{(A6.10)}$$

We used here trigonometric identity

$$\cos\alpha\sin\beta = \frac{1}{2}[\sin(\beta+\alpha)+\sin(\beta-\alpha)] \qquad \text{(A6.11)}$$

Integrating (A6.6) with this expression for the flux, one finds:

$$\begin{aligned} I = -\frac{B_0 w}{kL}\exp(-k\bar{y}_1)\{&\frac{1}{1+(R/\omega L)^2}\left[\sin(kz-\omega t)-\frac{R}{\omega L}\cos(kz-\omega t)\right]- \\ &-\frac{k\delta y_0}{2}\frac{1}{1+(R_+/\omega_+ L)^2}\left[\sin(kz-\omega_+ t)-\frac{R_+}{\omega_+ L}\cos(kz-\omega_+ t)\right]- \\ &-\frac{k\delta y_0}{2}\frac{1}{1+(R_-/\omega_- L)^2}\left[\sin(kz-\omega_- t)-\frac{R_-}{\omega_- L}\cos(kz-\omega_- t)\right]\} \end{aligned} \qquad \text{(A6.12)}$$

We add suffixes "+" and "-" to resistance R to show that, generally speaking, it may depends on frequency (as in the case of the flat track design where added resistance depends on frequency).

The magnetic field on the surface of the track, according to (4) and (A6.2), (A6.8) is (up to the terms linear in δy):

$$B_z = B_0\exp(-k\bar{y}_1)\left\{\sin(kz-\omega t)-\frac{1}{2}k\delta y_0[\sin(kz-\omega_+ t)+\sin(kz-\omega_- t)]\right\} \qquad \text{(A6.13)}$$

The average over the wavelength vertical force can now be found from equations (A6.12) and (A6.13). Retaining only the terms up to the first order in δy, and up to the first order in $R/\omega L$, one finds:

$$F_y \propto -\langle IB_z \rangle = \frac{B_0^2 w}{2kL}\exp(-2k\tilde{y}_1)\{1-$$
$$-2k\delta y_0\left[\langle \sin(kz-\omega_+ t)\sin(kz-\omega t)\rangle + \langle \sin(kz-\omega_- t)\sin(kz-\omega t)\rangle\right]-$$
$$-\frac{k\delta y_0}{L}\left[\frac{R_+}{\omega_+}\langle \cos(kz-\omega_+ t)\sin(kz-\omega t)\rangle + \frac{R_-}{\omega_-}\langle \cos(kz-\omega_- t)\sin(kz-\omega t)\rangle\right]- \quad \text{(A6.14)}$$
$$-\frac{k\delta y_0 R}{\omega L}\left[\langle \cos(kz-\omega t)\sin(kz-\omega_+ t)\rangle + \langle \cos(kz-\omega t)\sin(kz-\omega_- t)\rangle\right]\}$$

To take the averages, one can use relationships (A6.11) and

$$\sin\alpha\sin\beta = \frac{1}{2}[\cos(\alpha-\beta)-\cos(\alpha+\beta)] \quad \text{(A6.15)}$$

As a result, one obtains:

$$F_y = Mg\left[1-2k\delta y_0\cos\Omega t + \frac{k\delta y_0}{L}\frac{\partial}{\partial\omega}\left(\frac{R}{\omega}\right)\Omega\sin\Omega t\right] \equiv$$
$$\equiv Mg\left[1-2k\delta y - \frac{k}{L}\frac{\partial}{\partial\omega}\left(\frac{R}{\omega}\right)\delta\dot{y}\right] \quad \text{(A6.16)}$$

Here we used an approximation

$$\frac{R_+}{\omega_+}-\frac{R_-}{\omega_-} = 2\Omega\frac{\partial}{\partial\omega}\left(\frac{R}{\omega}\right) \quad \text{(A6.17)}$$

which implies that the oscillation frequency, Ω, is much less than the frequency of the current in conductors, $\omega=kv$.

Strictly speaking, our derivation pertains only to an infinitely long Halbach array. One can show, however, that it remains valid for relatively short arrays comprising several full wavelengths. We will not present here these rather lengthy derivations.

Substituting the perturbed part of the force into equation (A6.4), one finds an equation for small vertical oscillations, taking into account dissipative processes:

$$\delta\ddot{y} + \frac{kg}{L}\frac{\partial}{\partial\omega}\left(\frac{R}{\omega}\right)\delta\dot{y} + 2kg\delta y = 0 \quad \text{(A6.18)}$$

Assuming that the damping rate γ is small, one easily finds the following expression for γ (we define γ according to relationship $\delta y \propto exp(-\gamma t)$.):

$$\gamma = \frac{kg}{2L}\frac{\partial}{\partial\omega}\left(\frac{R}{\omega}\right) \qquad \text{(A6.19)}$$

For the window-frame design, in which resistance does not depend on frequency, one obtains:

$$\gamma = -\frac{g}{2\mathrm{v}}\frac{1}{K\mathrm{v}} \qquad \text{(A6.20)}$$

where K is a parameter defined by equation (18). As has been already mentioned, the damping is negative, i.e., the system is unstable.

The condition for applicability of our derivation requires that the growth-rate should be small compared to the eigenfrequency of the oscillations, equation (A6.5). This imposes the following constraint on the velocities for which equation (A6.20) is valid:

$$\mathrm{v} > (g/2K)^{1/2}(2kg)^{-1/4} \qquad \text{(A6.21)}$$

For K=2s/m and k=12.28 m^{-1} (λ=0.5 m), the r.h.s. of this inequality is approximately 0.35 m/s, that is, it is even lower than the critical velocity 1/K. In such a situation, the applicability condition for our analysis is just

$$\mathrm{v}>1/\mathrm{K} \qquad \text{(A6.22)}$$

For high speeds the growth rate of the instability, given by equation (A6.20), is very small and it can be easily stabilized, for example, by damping elements situated in the car. At slower speeds, in particular at the speeds not much greater than "critical" speed 1/K, without damping the growth rate would become significant. However at these speeds the back-up wheels will be engaged, damping the growth until inboard damping elements take over at higher speeds. Generally speaking, as the instability manifests itself only at low speeds, where many additional stabilization techniques based on the touch-down elements can be used, it should not be of serious concern.

The full dynamics of the system depends on the characteristics of the driving force. In the example we considered, this driving force was such as to provide constant-v motion of the car. In other situations, for instance in case when the driving force is constant, there will occur a peculiar coupling of the translational motion and vertical oscillations. This and the other issues of the similar nature will be considered in our forthcoming report [8].

Appendix 7.

Optimization of the Ratio of Levitated Weight Relative to Magnet Weight

In some applications of the Inductrack concept, for example in its use in a high-speed test track, it becomes important to maximize the ratio of the levitated weight to the weight of the magnets. For such applications the Lift/Drag ratio may be a less important parameter, so that maximizing the lift through elimination of extra inductive loading is an appropriate path. In this case the use either of a "flat track" design or of a conductive surface can be considered, as these permit maximization of the lifting force per unit area. We here consider the problem of maximizing the ratio of levitated weight relative to the weight of the magnets in the Halbach arrays through optimal choice of the thickness, d m., of the magnets, of the number of magnet segments, M, per wavelength, and of the wavelength, λ m., of the arrays.

For the case of an optimized "flat" track, equation (29) gives an expression for the force per unit area in the limit of high speed ($\omega L/R \gg 1$):

$$\frac{\Sigma\langle F_y^{max}\rangle}{A} = \left[\frac{B_0^2}{\mu_0}\right] \exp(-2ky_1 - k\Delta_c) \quad N/m \qquad (A7.1)$$

Here B_0 is defined as before, in terms of B_r, d, and M, through the expression:

$$B_0 = [1 - \exp(-kd)]\left[\frac{\sin(\pi/M)}{\pi/M}\right] B_r \quad Tesla \qquad (A7.2)$$

The magnet mass per unit area is given by ρd kg/m. It follows that we can write for the ratio of the levitated weight to the magnet weight the following expression:

$$\frac{\text{Wt. lev.}}{\text{Wt. of mag.}} = \frac{B_r^2 k}{\mu_0 g \rho}\left[\frac{\sin(\pi/M)}{\pi/M}\right]^2 G(kd)\ \exp(-2ky_1 - k\Delta_c) \qquad (A7.3)$$

where

$$G(x) = \frac{[1-\exp(-x)]^2}{x} \qquad (A7.4)$$

The function G(kd) describes the competition between the increased levitation that accompanies the use of thicker magnets and the increased mass of magnet material associated with thicker magnets. As shown in Fig. (18) this function varies only slowly in the vicinity of its maximum value (0.4073) which occurs at kd = 1.256 (i.e., at a magnet thickness corresponding to 0.1999 λ). It remains within 10 percent of its maximum value between kd = 0.7 and kd = 2.1, i.e., a factor of 3 in kd values between the extremes. Values of kd near the lower limit imply the need for larger areas of magnets to accomplish the same lifting force (relative to the optimum value); kd values near the upper limit imply the opposite.

If we now choose M = 8 (to approach the maximally efficient Halbach array: $M \rightarrow \infty$), insert the density, ρ = 7500 kg/m, adopt the maximum value for G(kd), and insert the other constants into equation A7.3, we then arrive at an expression for the maximum value of the ratio of levitated weight to magnet weight given by:

$$\left[\frac{\text{Wt. lev.}}{\text{Wt. mag.}}\right]_{\max(kd)} = 26.31\left[\frac{B_r^2}{\lambda}\right](\exp[-2k(y_1-\Delta_c/2)] \qquad (A7.5)$$

In any given application there remains one more parameter to vary in order to achieve the maximum possible value of this ratio. This parameter is the wavelength of the Halbach array, which appears in two places in the above equation, namely, in the denominator and in the exponential term, through $k = 2\pi/\lambda$. We will illustrate this last optimization for the case that gives the maximum possible value of the parameter, i.e., when the Inductrack is replaced

by a conducting surface, represented by setting the term $\Delta_c = 0$. Here our equation for the maximized ratio as function of λ and y_1 becomes

$$\left[\frac{\text{Wt. lev.}}{\text{Wt. mag.}}\right]_{\max(kd)} = 26.31\ B_r^2 H(\lambda, y_1) \qquad \text{(A7.6)}$$

where

$$H(\lambda, y_1) = \{\exp[-4\pi y_1/\lambda]\}/\lambda \qquad \text{(A7.7)}$$

For a given value of y_1, the maximum value of $H(\lambda, y_1)$ occurs at a wavelength

$$[\lambda]_{\text{optimum}} = 4\pi y_1 \quad \text{m.} \qquad \text{(A7.8)}$$

The corresponding maximized value of $H(\lambda, y_1)$ is therefore

$$[H(\lambda, y_1] = \exp(-1)/(4\pi y_1) = .02928/y_1 \qquad \text{(A7.9)}$$

Inserting this optimized value into equation (A7.6) we therefore find

$$\left[\frac{\text{Wt. lev.}}{\text{Wt. mag.}}\right]_{\max(kd,\lambda)} = 0.7702\ B_r^2/y_1 \qquad \text{(A7.9)}$$

There is now available a NdFeB magnet material for which B_r = 1.41 Tesla. If we insert this value into equation (A7.9) we find an expression for the best ratio of levitated weight to magnet weight that is presently achievable for the system we have described. This value is

$$\left[\frac{\text{Wt. lev.}}{\text{Wt. mag.}}\right]_{\max(kd,\lambda)} = 1.53/y_1 \qquad \text{(A7.10)}$$

The value of y_1 that can be used will depend, of course, on the application. For a high-speed test track a typical value might be .03 m. In this case we find for the optimum wavelength

the value $[\lambda]_{optimum} = 4\pi y_1 = .377$ m, and for the ratio of levitated weight to magnet weight the value

$$\left[\frac{\text{Wt. lev.}}{\text{Wt. mag.}}\right]_{max(kd,\lambda)} = 51.$$

Thus to sustain a downward force of, say 5 metric tonnes (11,000 lbs) would require Halbach arrays weighing a total of 98 kilograms. The maximum upward force that these arrays could then exert (for a magnet-to-track gap, y_1, approaching zero) would be, from equation A7.6, equal to 13.6 metric tonnes (30,000 lbs.).

For the case of a flat Inductrack where the vertical depth of the conductors of the track is a fixed fraction of the wavelength, i.e., where $\Delta_c = \varepsilon\lambda$, the optimum wavelength remains the same as before, but the expression for the ratio of the levitated weight to the magnet weight is multiplied by a term $\exp(-2\pi\varepsilon)$ so that we have

$$\left[\frac{\text{Wt. lev.}}{\text{Wt. mag.}}\right]_{max(kd,\lambda)} = 1.53\ [\exp(-2\pi\varepsilon)/y_1] \qquad \text{(A7.11)}$$

For the case considered before, with $\varepsilon = 1/16$, and for $y_1 = .03$ m., we then have

$$\left[\frac{\text{Wt. lev.}}{\text{Wt. mag.}}\right]_{max(kd,\lambda)} = 34.4$$

Because of the exponential dependence of this ratio on the thickness of the conductor it may be advantageous in some situations to use a smaller value of Δ_c in return for a closer approach to the limiting value. For example, choosing $\varepsilon = 1/32$ results in a value

$$\left[\frac{\text{Wt. lev.}}{\text{Wt. mag.}}\right]_{max(kd,\lambda)} = 46.2$$

which is 91 percent of the limiting value, while still retaining a much higher value of L/D at high speeds than that for a conducting surface.

Appendix 8.
Traction System

We remind the reader that the lumped inductance incorporated into every conductor is conceived as a cylinder of a high-μ material (made of thin laminations, to reduce eddy current losses) which (cylinder) surrounds a short section of a conductor (see Figs. 2, 5). We now assume that each cylinder is threaded with another winding attached to the external source of voltage which creates a periodic electromotive force

$$E=E_0 sin(\omega t+\varphi) \tag{A8.1}$$

with the frequency coinciding with that excited in the conductor by the moving car. In other words, we assume that the equality $\omega=kv$ holds. For the first rough assessment, we characterize this external circuit by its resistance r and do not include possible capacitive or (additional) inductive elements which may be present in this circuit. We also assume that inductive coupling between the two circuits is perfect. This means that, if the flux (through the laminations) linked with the current in the track conductor is ϕ, then the flux through the external circuit is $N\phi$ where N is the number of turns of the external winding (Fig. 19).

The circuit equations describing interaction of the two circuits are:

$$\begin{aligned} \left(L+L^{(d)}\right)\dot{I}+RI &= -\dot{\phi}-NL\dot{I}_{ext} \\ N\left(NL\dot{I}_{ext}+L\dot{I}\right)+rI_{ext} &= E_0\sin(\omega t+\varphi) \end{aligned} \tag{A8.2}$$

here ϕ is the magnetic flux induced by the Halbach array, $\phi=\phi_0\sin(\omega t)$ (Cf. equation (1)), while I_{ext} is a current in the external circuit. By L we mean the lumped inductance (as in equation (1)) and by $L^{(d)}$ the distributed inductance, equation (21). In the case of small Ohmic losses (which is of maximum practical importance), resistive terms in these equations can be neglected in the first approximation. Then equations (A8.2) yield:

$$\begin{aligned} I &= -\frac{\phi_0\sin\omega t}{L^{(d)}}+\frac{E_0\cos(\omega t+\varphi)}{\omega NL^{(d)}} \\ I_{ext} &= \frac{\phi_0\sin\omega t}{NL^{(d)}}-\frac{E_0}{\omega N^2}\left(\frac{1}{L^{(d)}}+\frac{1}{L}\right)\cos(\omega t+\varphi) \end{aligned} \tag{A8.3}$$

Using relationships (4), (5) and (9) and taking the average, one finds for the force per conductor:

$$\langle F_y \rangle = \frac{B_0^2 w^2}{2kL^{(d)}} e^{-2ky_1 - k\Delta_c} + \frac{E_0 B_0 w}{2NL^{(d)}\omega} e^{-ky_1 - k\frac{\Delta}{2}} \sin\varphi$$
$$\langle F_z \rangle = \frac{E_0 B_0 w}{2NL^{(d)}\omega} e^{-ky_1 - k\frac{\Delta}{2}} \cos\varphi \qquad \text{(A8.4)}$$

Maximum traction force $<F_z>$ corresponds to the phase shift $\varphi = 0$. One can note in passing that in this case there is no interference between the lift and the traction force.

External voltage in the neighboring external circuits (exciting the neighboring conductors) should have a relative phase shift equal to 2π divided by the number of conductors per wavelength (16 in our base case discussed on p.15). This means that a multi-phase power supply system will be required. Use of an 8-phase power supply, with the voltage for two neighboring circuits having the same phase, is also conceivable (if a 16-phase power supply poses too challenging of an engineering problem).

The maximum traction force corresponding to the phase shift $\varphi = 0$, can be conveniently related to the lifting force:

$$\frac{\langle F_z \rangle}{\langle F_y \rangle}\Big|_{\varphi=0} = \frac{E_0}{vwB_0} e^{ky_1 + k\frac{\Delta}{2}} \qquad \text{(A8.5)}$$

For the parameters of the Grumman design of the car, the ratio of the aerodynamic drag to the weight is approximately 0.13 (7 tonnes vs 50 tonnes). For $B_0 \sim 1$ T, $v \sim 150$ m/s, $w = 1$m, the required electromotive force E_0 which can be evaluated from equation (A8.5), is in the range of 50 V.

To make the system stable with respect to possible slight variations of the drag force, one should operate the system at ϕ different from zero. For ϕ=30 degrees, the reduction of the traction force is approximately 15% with respect to the maximum value.

The phase velocity of the driving wave should closely concide with the velocity of the car - otherwise the "sliding" of the wave with respect to the car will occur. The upper limit of the velocity

mismatch can be evaluated from the condition

$$\Delta v << (drag\,force/car\,weight)^{1/2}(g/k)^{1/2} \qquad \text{(A8.6)}$$

For $drag/weight$ =0.13 and the wavelength λ=1m, one finds that the r.h.s. of the inequality is equal to 0.4 m/s.

Generally speaking, the presence of the external circuit affects the lift and drag forces. For instance, the first of the equations (A8.4) shows that the lift force contains now only the distributed inductance $L^{(d)}$ and not the total inductance as was the case when there was no external circuit.(Cf. equation (22)).

Now we evaluate the Ohmic losses in the system. Assuming that the they are small, one can find them from a simple expression:

$$P_{loss} = R\langle I^2\rangle + r\langle I_{ext}^3\rangle \qquad \text{(A8.7)}$$

(per conductor). For small drag/weight ratios, one can neglect the last terms in the expression (A8.3) compared to the first ones, thereby arriving at the following expression for the losses:

$$P_{loss} = \frac{\phi_0^2}{2L^{(d)2}}\left(R + \frac{r}{N^2}\right) \qquad \text{(A8.8)}$$

The presence of the factor $1/N^2$ in the term responsible for the Ohmic losses in the external circuit shows that a relatively high resistance of this circuit is permitted; accordingly, the use of litz wire may be unnecessary in the external circuit.

In case of the "flat" track design, the current providing the traction force can be excited directly (not inductively) through the cuts in every conductor, as shown in Fig. 20. Expressions equivalent to equation (A8.4) in this case read:

$$\begin{aligned}\langle F_y\rangle &= \frac{wB_0 e^{-ky_1-\frac{\Delta_c}{2}}}{2L\omega}\left(B_0 v w e^{-ky_1-\frac{\Delta_c}{2}} + E_0\sin\varphi\right)\\ \langle F_z\rangle &= \frac{wB_0E_0 e^{-ky_1-\frac{\Delta_c}{2}}}{2L\omega}\cos\varphi\end{aligned} \qquad \text{(A8.9)}$$

In both schemes, the traction force depends on the distance between the car and the track. This shows that, generally speaking,in the stability analysis of the car motion, one should take into acount the coupling between vertical and horizontal oscillations.

The scheme for a power supply to the traction circuits could be as follows: There could be a power line (Dc or 60 Hz) along the track; the feeds from it could be branched to the sections of 2-3 car lengths (for a 30 m car, every 60-100 m), containing a few hundreds of track conductors and external circuits. Each section should be engaged just before the car enters it and be disengaged as soon as the car leaves it; every section should have a converter that would provide a periodic voltage of a desired frequency and amplitude during the passage of the car.

One could also use an alternative system in which capacitive or inductive energy storages would be attached to every section of the track. One could then charge them slowly in advance, when the car is approaching, and discharge them quickly, through the LC contour which would allow to adjust the frequency of oscillations (tunable elements will be required; mechanical tuning is probably possible). One should remember that for the friction force of 70,000 N (discussed in the text), one should store approximately 70 kJ of energy per one meter of the track. Cost-wise, this would probably give an advantage to the inductive energy storages.

Appendix 9:
Minimum Value of the Design Parameter, "K"

The parameter K, Newtons/Watt (or sec./m.) is an important quantity in the design of Inductrack systems. It is defined, through Equation (18) of the text and what follows, by the relationship

$$K = \frac{2\pi\left[L+L^{(d)}\right]}{\lambda R} \quad \text{Newtons/Watt} \qquad \text{(A9.1)}$$

Here, as noted before, the inductance term includes both the inductance added to each circuit by ferromagnetic elements, L, and the distributed-inductance term, $L^{(d)}$, arising from the

presence of adjacent circuits. The term $L^{(d)}$ is defined by Equation (21) of the text

$$L^{(d)} = \frac{\mu_0 P_c}{2kd_c} \quad hy \qquad (A9.2)$$

Here P_c is the perimeter of a coil, and d_c is the axial length of the conductor bundle of the coil.

In the design of an Inductrack system it is important to determine the minimum value of the parameter K, occuring when there is no added inductive loading. Thus we have

$$K_{min} = \frac{2\pi L^{(d)}}{\lambda R} \quad \text{Newtons/Watt} \qquad (A9.3)$$

This quantity is also useful for determining the maximum lifting force obtainable from an Inductrack system, as compared to the theoretical maximum (see Equation 30 of the text).

The expression for K_{min} can be simplified, and made easier to apply, if we insert the definitions for $L^{(d)}$ and R into Equation (A9.3). The resistance term, R can be defined in terms of the length of the circuit, P_c (m.), the axial length of the circuit, d_c(m.), its depth, Δ_c (m.), and the resistivity, ρ (ohm-m.), and the packing fraction, f, of its windings. We have

$$R = \frac{\rho P_c}{f\Delta_c d_c} \quad \text{ohms} \qquad (A9.4)$$

Inserting these definitions into Equation A9.3 we find the expression:

$$K_{min} = \frac{\mu_0 f \Delta_c}{2\rho} \quad \text{Newtons/Watt} \qquad (A9.5)$$

Note that K_{min} is independent of the overall scale of the system, depending only on the packing fraction and depth of the windings and the resistivity of the material from which they are fabricated.

As an example, consider an Inductrack system made of copper windings (ρ = 1.7 x 10^{-8} ohm-m.) with a packing fraction f = 0.8 and a depth, Δ_c, of 0.03125 m. (as in the examples summarized in Section VII). From Equation A9.5 we then find K_{min} = 0.92 Newtons/Watt.

TABLES

TABLE 1

Parameters of the Inductrack system for several design options for the case K=1 s/m.

	Window-frame, copper	Window-frame, aluminum	Window-frame, aluminum	Flat, copper	Flat, aluminum
Spatial period of the Halbach array, λ, m	0.5	0.5	1.0	0.5	0.5
Perimeter of the conductor, P_c, m	3.0	3.0	3.0	1.2	1.2
Weight of the conductor, T/m^2	0.67	0.2	0.2	0.27	0.081
Resistance of the conductor, R, μOhm	65	105	105	26	42
Added resistance of the bus-bars at the speed v=140 m/s, R_{Add}, μOhm	0	0	0	11	11
Distributed inductance, $L^{(d)}$ μHy	4.8	4.8	9.6	1.9	1.9
Lumped inductance, L, μHy	0.4	3.6	7.2	0.2	1.5
Lifting force at high speed, T/m^2 *)	6.2 (9.3)	3.8 (5.7)	3.2 (4.8)	15.1 (27.7)	9.3 (13.9)

*) Shown in brackets are the values of lifting force for a more advanced Halbach array, with M=8 and B_r=1.41 T

TABLE 2

Parameters of the Inductrack system for several design options for the case K=2 s/m.

	Window-frame, copper	Window-frame, aluminum	Window-frame, aluminum	Flat, copper	Flat, aluminum
Spatial period of the Halbach array, λ, m	0.5	0.5	1.0	0.5	0.5
Perimeter of the conductor, P_c, m	3.0	3.0	3.0	1.2	1.2
Weight of the conductor, T/m^2	0.67	0.2	0.2	0.27	0.081
Resistance of the conductor, R, μOhm	65	105	105	26	42
Added resistance of the bus-bars at the speed v=140 m/s, R_{Add}, μOhm	0	0	0	11	11
Distributed inductance, $L^{(d)}$ μHy	4.8	4.8	9.6	1.9	1.9
Lumped inductance, L, μHy	5.5	11.9	23.9	2.3	4.8
Lifting force at high speed, t/m^2	3.1 (4.7)	1.9 (2.9)	1.6 (2.4)	7.6 (11.4)	4.7 (7.1)

*) Shown in brackets are the values of lifting force for a more advanced Halbach array, with M=8 and B_r=1.41 T

References

1. R.F. Luerkin, "Trans Rapid - The First High-Speed Maglev Train System Certified and Ready for Application: Development Status and Prospects for Development", Proceedings of the Second International Symposium on Magnetic Suspension Technology, Seattle, Washington, August 1113, 1993, NASA Conference Publication, 3247, Part 5, p.77.

2. J.R. Powell and G.R. Danby, "Magnetic Suspension for Levitated Tracked Vehicle", Cryogenics, Vol. 11, (1971) pp. 192204.

3. R.F. Post, "Magnetic Levitation System for Moving Objects" (patent pending).

4. S.S. Kalsi, "Superconductive Electromagnetic Suspension for Grumman Maglev Concept", Proceedings from the Second International Symposium on Magnetic Suspension Technology, Seattle, Washington, August 1113, 1993, NASA Conference Publication, 3247, Part 5, p.197.

5. R. Halbach, "Application of Permanent Magnets in Accelerators and Electron Storage Rings", *Journal of Applied Physics*, **57** (1985) 3605.

6. S.S. Kalsi, "Superconductive Electromagnetic Suspension for Grumman Maglev Concept", Proceedings from the Second International Symposium on Magnetic Suspension Technology, Seattle, Washington, August 1113, 1993, NASA Conference Publication, 3247, Part 5, p.197.

7. J.D. Jackson, Classical Electrodynamics, Wiley, (1975).

8 R.F. Post and D.D. Ryutov, "The Inductrack Concept: Linear Stability Theory" (in preparation).

Figure Captions

Fig 1 (Sec. II, p.6) Schematic representation of the Inductrack concept.

Fig.2 (Sec.IV, p.7) Schematic of the "window-frame" track design. The Halbach array will be situated above y=0 plane and will move in z-direction, parallel to the track surface. Shown in dotted lines are inductive elements enclosing every conductor. To provide space for this elements, the lower parts of neighboring conductors are shifted in the vertical direction with respect to each other.

Fig.3 (Sec.IV, p.8) Periodic array of permanent magnet bars

Fig.4. (Sec.IVA, p.9) The equivalent circuit of one circuit of the Inductrack circuit

Fig.5 (Sec.VB, p.22) Schematic of the "flat" track design. Shown are two of the conductors forming the track. The ends of the conductors are slightly bent in opposite directions to provide space for accomodating the rings of the laminated high-μ material (lumped inductances). The bus bars are shown as flat surfaces at the left and at the right.

Fig.6 (Sec.VB, p.22) Litz-type structure of the conductor for the "flat" track design. Shown are two of many hundreds or even thousands of insulated wires which wonder between the upper and the lower surface of the conductor. The scale is not observed: the transverse dimension of the conductor is exaggerated. In reality, the wires will form a considerably smaller angle with the horizontal direction. Two wires (thin solid and dashed lines on the figure), in the points of their apparent intersection are, in fact, slightly displaced with respect to each other in the direction normal to the figure. This type of winding forces the average current (averaged over many wires) to be almost uniform over the conductor.

Fig.7 (Sec.VC, p.25) The track in the form of a conducting slab. Slab thickness, Δ_c, is assumed to be greater than the skin-depth δ. The width of the slab is greater than the width of the Halbach array.

Figs.8a and 8b
(Sec.VC, p.25) Velocity dependence of lift force and lift-to-drag ratio in the "slab" design. It is assumed that the track is made of copper and the wavelength of the Halbach array is λ=0.5 m. The vertical line corresponds to the velocity v=2.2 m at which the skin-depth δ becomes equal to the slab thickness ($\Delta_c = \lambda/16$)

Fig. 9 (Sec. VII, p.29) The velocity dependence of the lift-to-drag ratio for two Inductrack cases (K = 3.0 and K = K_{min}) compared to that for a conducting plate.

Fig. 10 (Sec. VII, p.29) The velocity dependence of the levitation force vs its limiting value (for $v >> v_{transition}$ for the case K = K_{min}.

Fig. 11 (Sec. VII, p.29) The velocity dependence of the levitation force vs its limiting value (for $v >> v_{transition}$ for the case K = 3.0. Note the low value of the transition speed (1.2 km/hr).

Fig. 12 (Sec. VII, p.29) Plot of the decrease of levitation force with height above the Inductrack, for the case λ = 1.0 meter.

Fig. 13 (Sec. VII, p.29) Block graph plot of the power required for levitation for three cases: (1) an Inductrack with K = 3.0, (2) an Inductrack with K = K_{min}, and, (3) a conducting plate track.

Fig. 14 (Sec. VII, p.29) Block graph plot of the maximum levitated mass in tonnes/m^2 for (1) a conducting plate, (2) an Inductrack with K = K_{min}, and (3) and Inductrack with K = 3.0. For comparison the calculated value of the mass/m^2 of the Halbach array magnets (for magnets λ/4 in thickness) is also shown. In these plots the wavelength is 1.0 meter and the value of B_0 is 1.0 Tesla.

Fig.15 (Appendix 4, p.38) Cross-section of M=4 Halbach array. The array is moving in the direction z>0. Double arrows indicate the directions of magnetization of every rod; encircled dots and crosses indicate the direction of the magnetization current.

Fig.16 (Appendix 4, p.39) Schematic of the zone where the track surface intersects the bus-bar. Both the track thickness and small bends of the ends of the conductors (see Fig.5) are neglected on this figure. Arrows show the current pattern.

Fig.17 (Appendix 5, p.41) Towards evaluation of the eddy-current losses in the separate wires. Shown on the figure are strongly magnified meridional (above) and equatorial (below) cross-sections of the separate wire in the flat-track conductor. We neglect small wiggles of the wire in y-direction (Fig.) and present a model of the wire "rectified" in the x-direction. Small deviations of a real wire from a straight line give rise to corrections of order $\alpha^2 << 1$ where α is an angle of a particular stretch of the wire with respect to axis x (Fig.).

Fig. 18 (Appendix 7, p.50) Plot of the function G(x) encountered in the maximization of the levitated mass relative to the mass of the magnets.

Fig. 19 (Appendix 8, p.53) Inductive excitation of the traction force. External electromototive force $E_0 \sin(\omega t+\phi)$ is applied to a circuit which is threaded N times through ferritic laminations (the latter serve also as a lumped inductance for the levitation current).

Fig. 20 (Appendix 8, p.55) Direct excitation of the the traction force in the flat-track design. External electromotive force $E_0 \sin(\omega t+\phi)$ is applied to the cut in the conductor. The exact location of the cut is not important and can be chosen to satisfy other possible design/economics constraints.

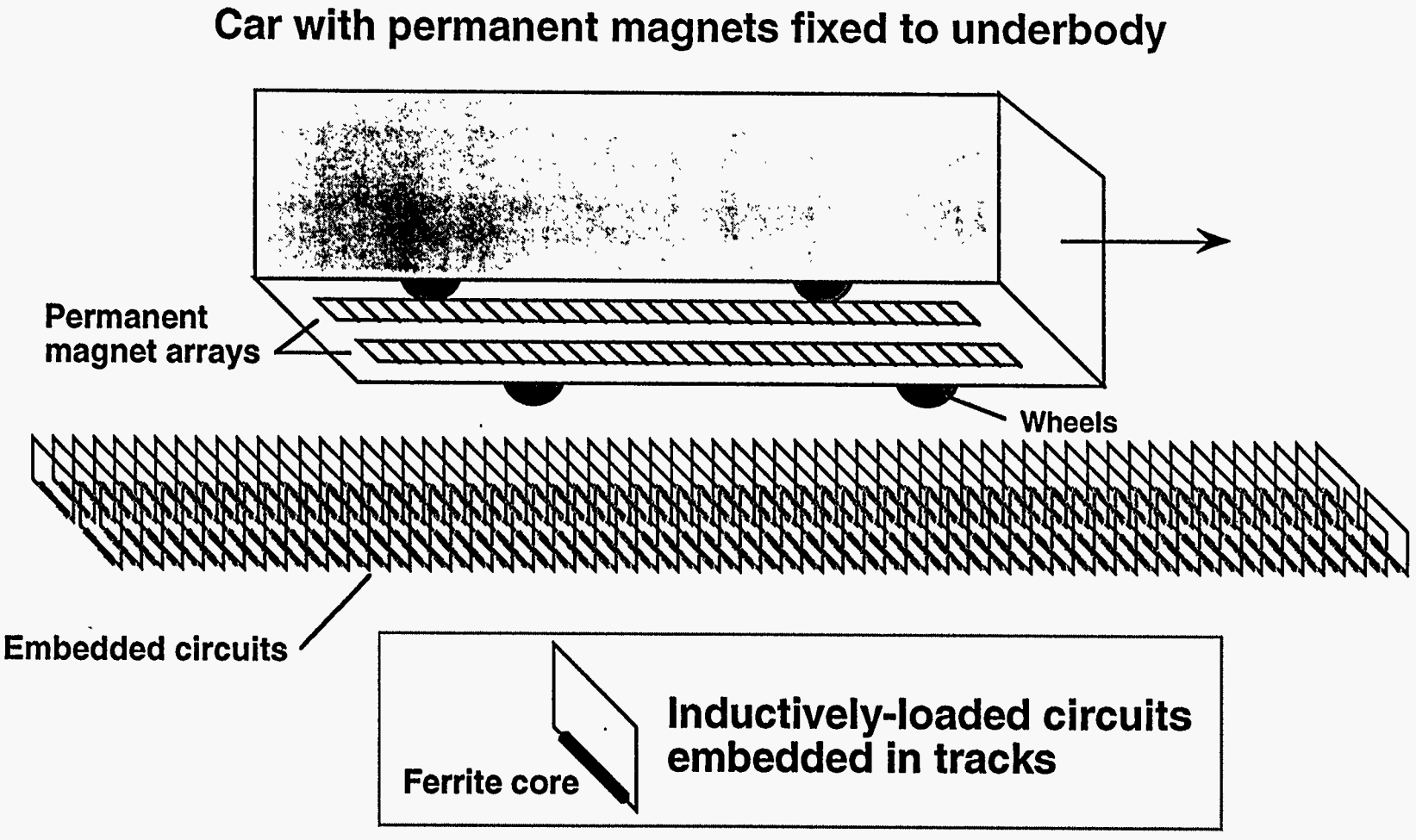
Car with permanent magnets fixed to underbody
Permanent magnet arrays
Wheels
Embedded circuits
Ferrite core
Inductively-loaded circuits embedded in tracks

Figure 1

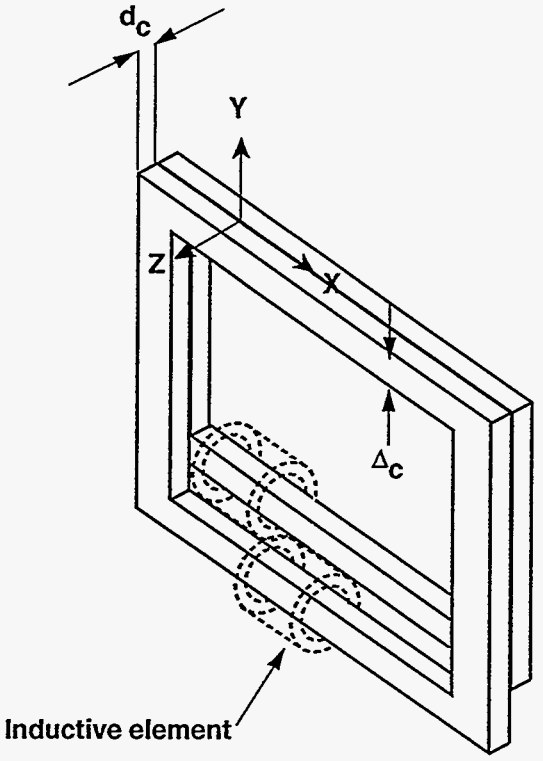

Figure 2

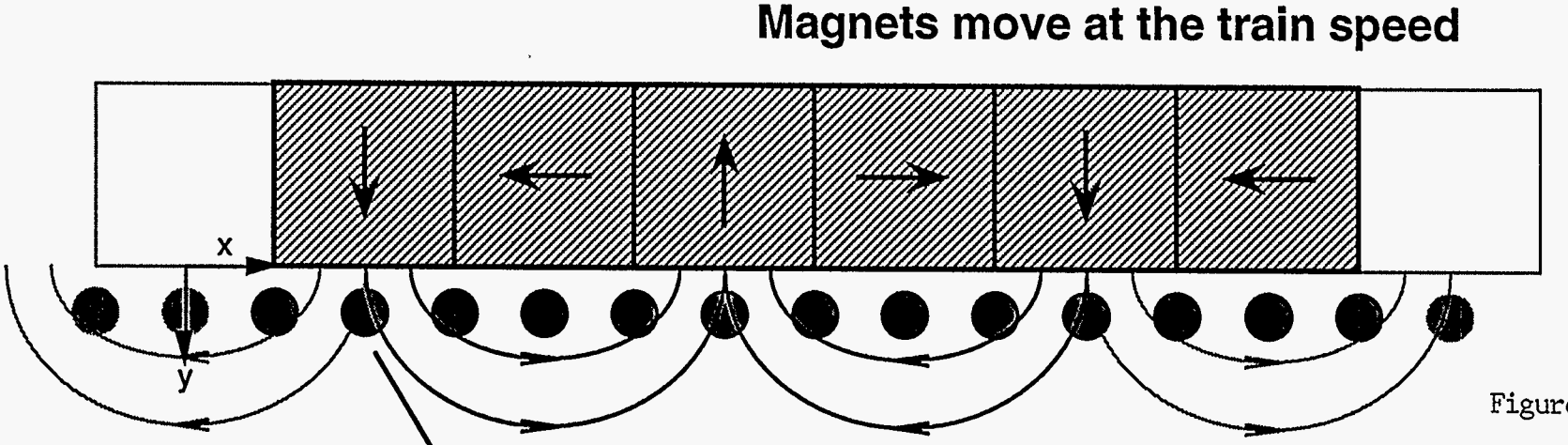

Figure 3

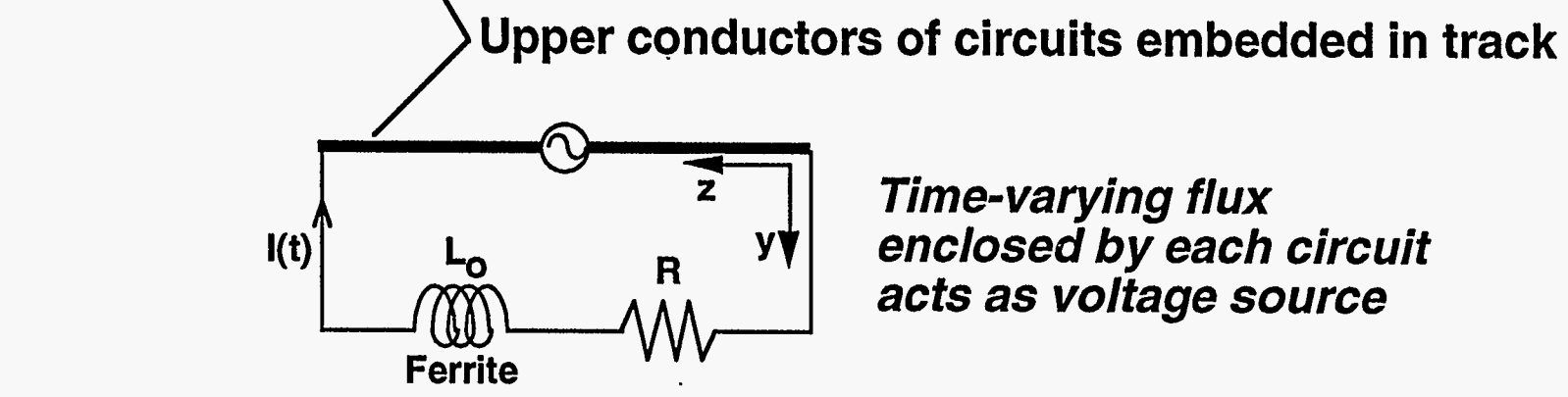

Figure 4

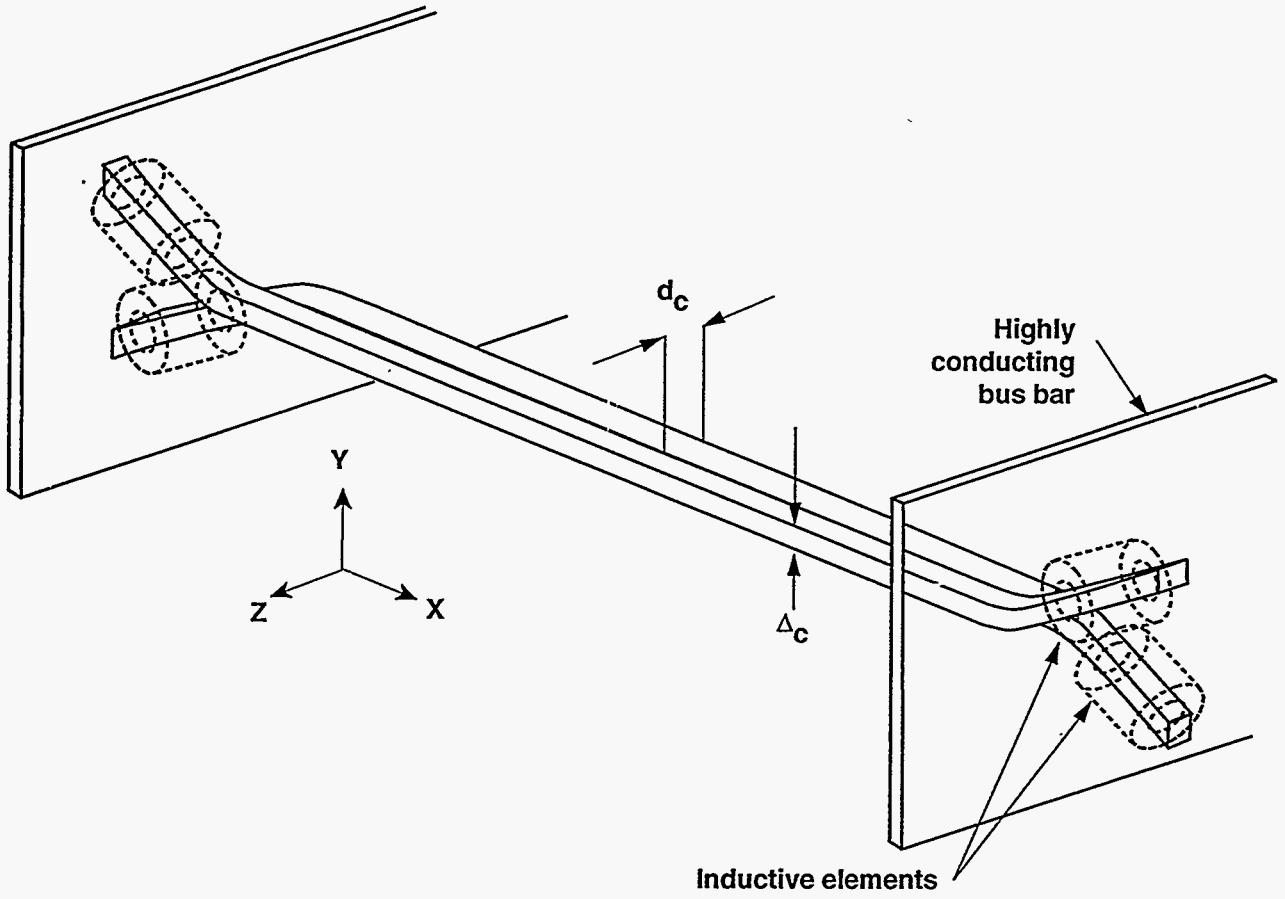
d_c
Highly
conducting
bus bar
Y
Z
X
Δ_c
Inductive elements

Figure 5

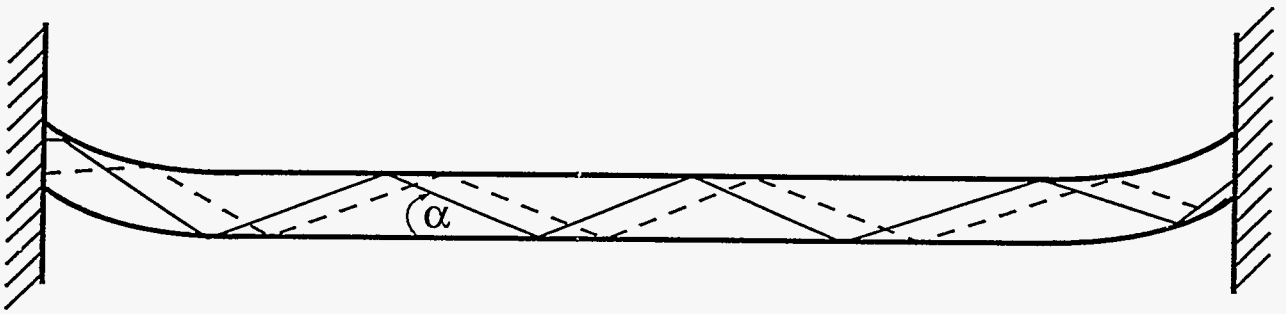

Figure 6

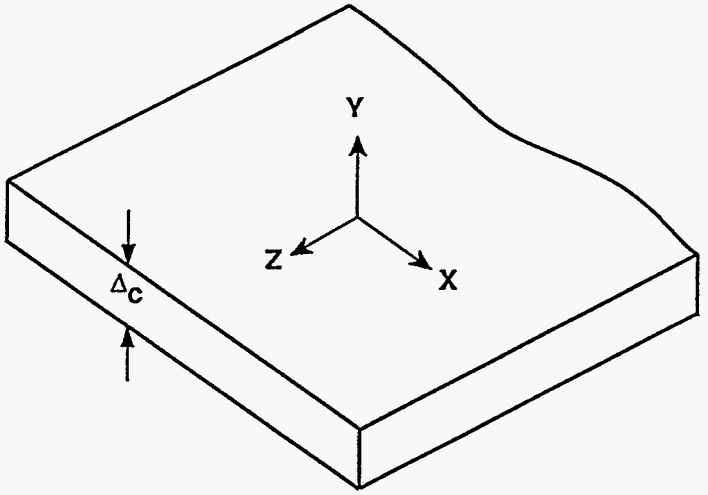

Figure 7

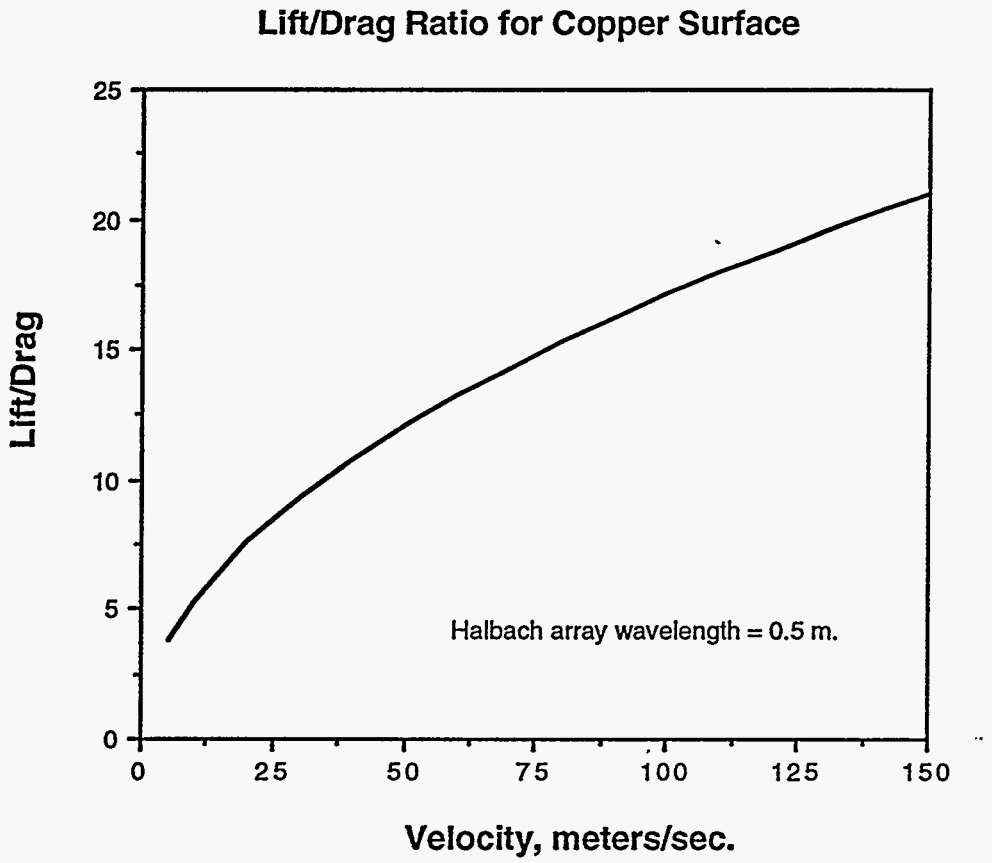
Lift/Drag Ratio for Copper Surface
Lift/Drag
25
20
15
10
5
0
0
25
50
75
100
125
150
Halbach array wavelength = 0.5 m.
Velocity, meters/sec.

Figure 8a

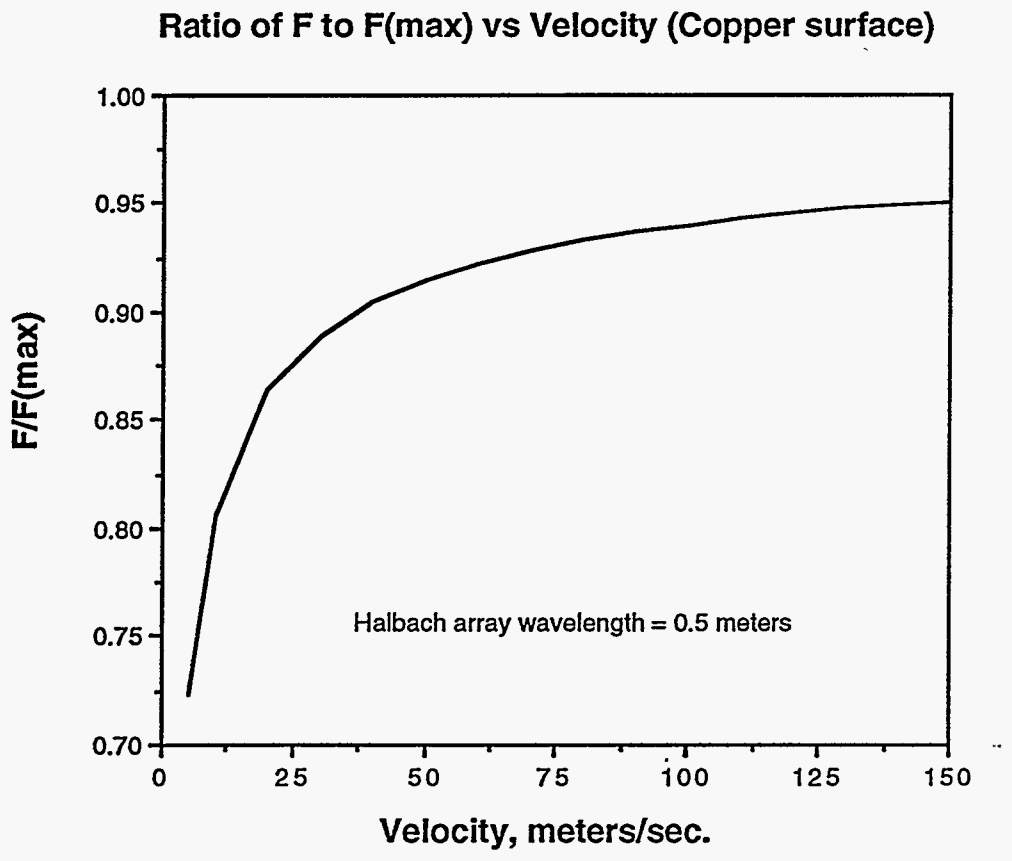
Ratio of F to F(max) vs Velocity (Copper surface)
F/F(max)
1.00
0.95
0.90
0.85
0.80
0.75
0.70
0
25
50
75
100
125
150
Velocity, meters/sec.
Halbach array wavelength = 0.5 meters

Figure 8b

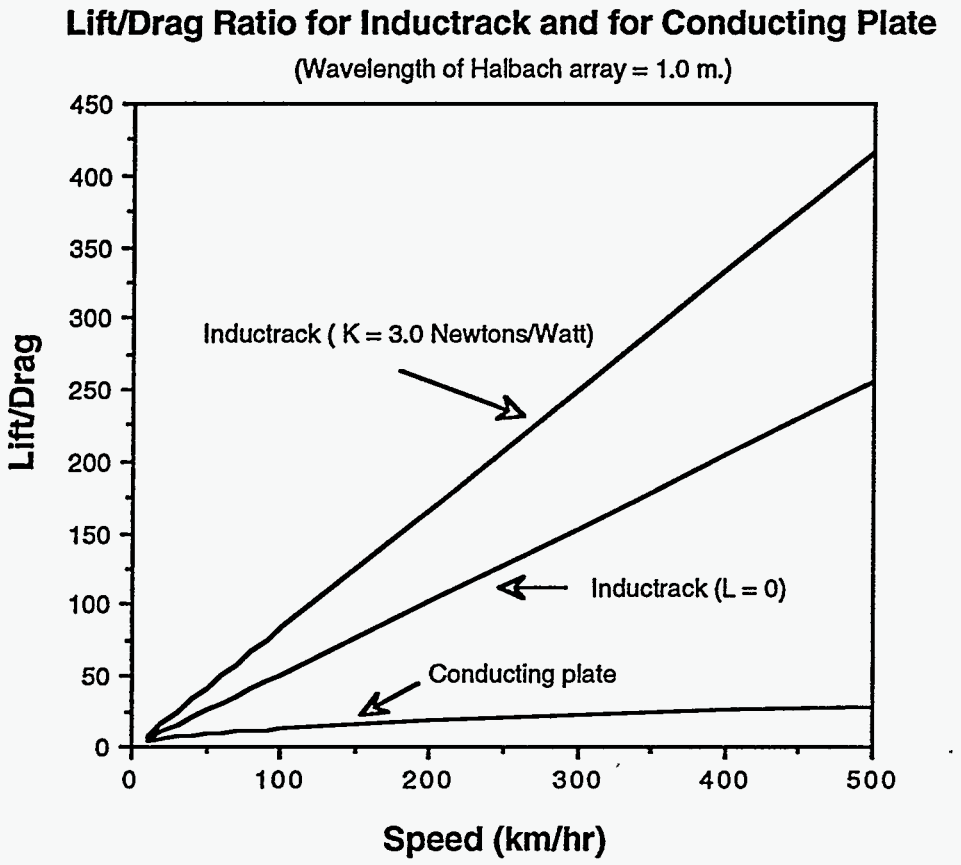
Lift/Drag Ratio for Inductrack and for Conducting Plate
(Wavelength of Halbach array = 1.0 m.)
Lift/Drag
450
400
350
300
250
200
150
100
50
0
Inductrack (K = 3.0 Newtons/Watt)
Inductrack (L = 0)
Conducting plate
0
100
200
300
400
500
Speed (km/hr)

Figure 9

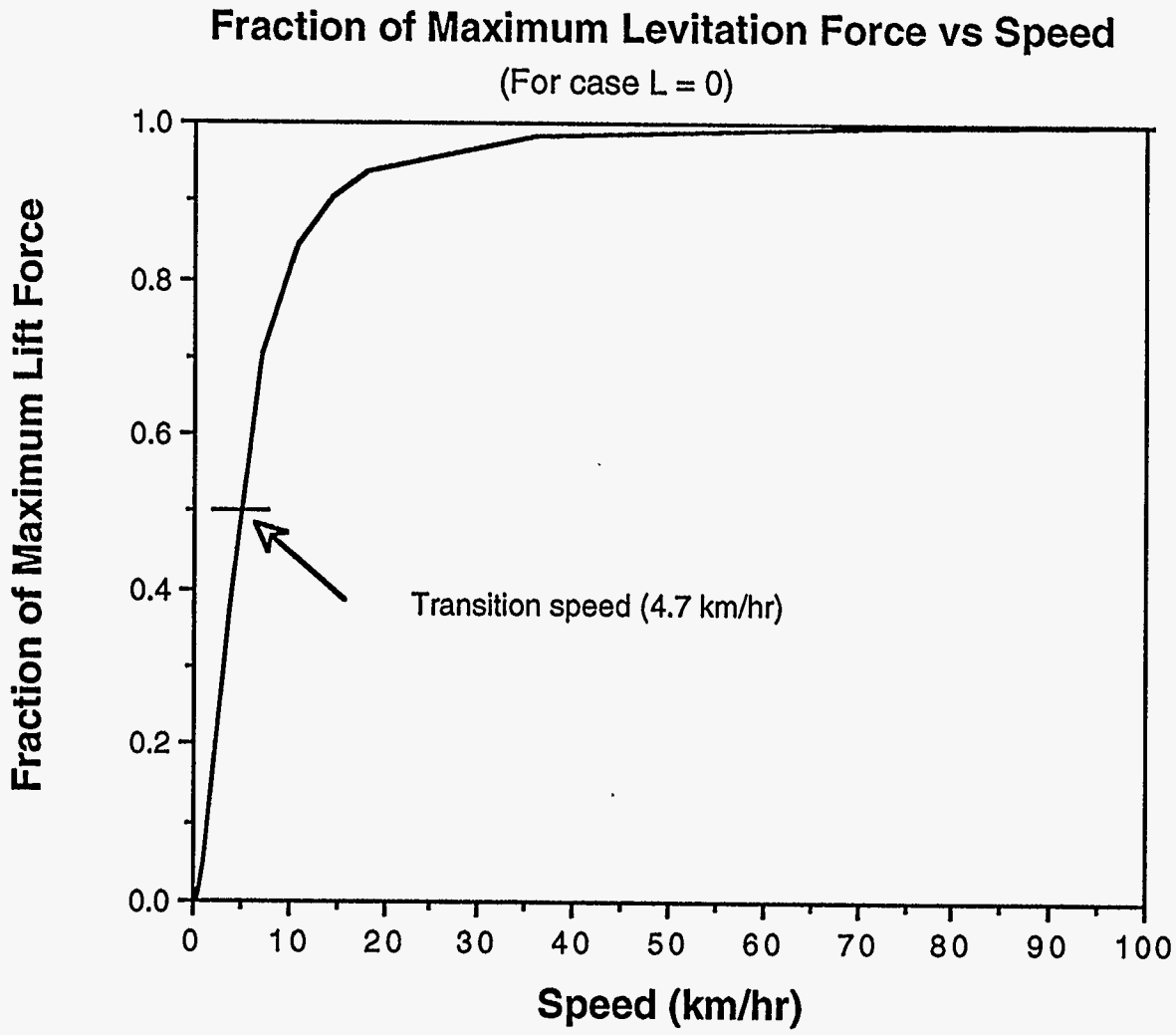
Fraction of Maximum Levitation Force vs Speed
(For case L = 0)
Fraction of Maximum Lift Force
1.0
0.8
0.6
0.4
0.2
0.0
Transition speed (4.7 km/hr)
0
10
20
30
40
50
60
70
80
90
100
Speed (km/hr)

Figure 10

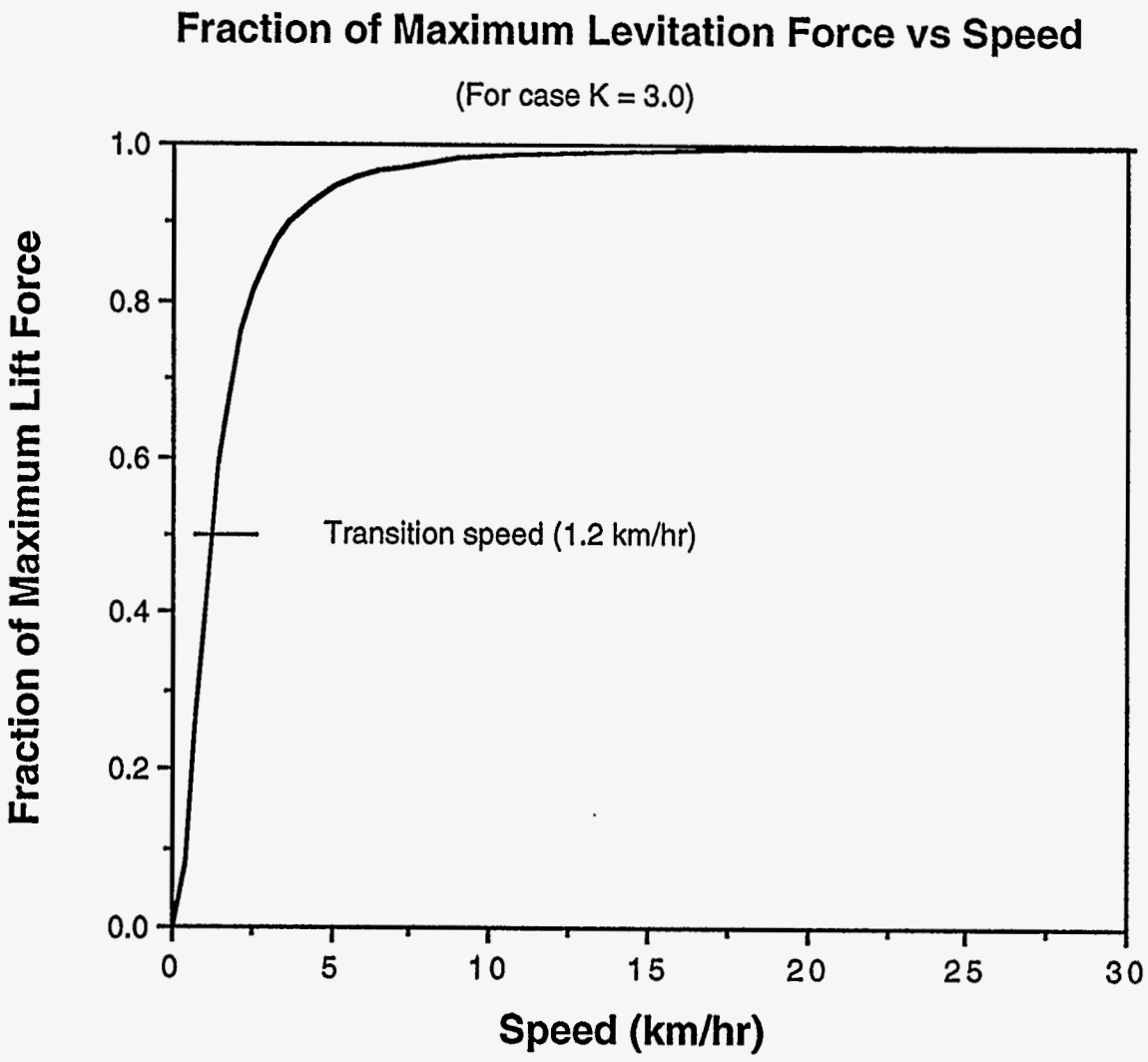
Fraction of Maximum Levitation Force vs Speed
(For case K = 3.0)
Fraction of Maximum Lift Force
1.0
0.8
0.6
0.4
0.2
0.0
Transition speed (1.2 km/hr)
0
5
10
15
20
25
30
Speed (km/hr)

Figure 11

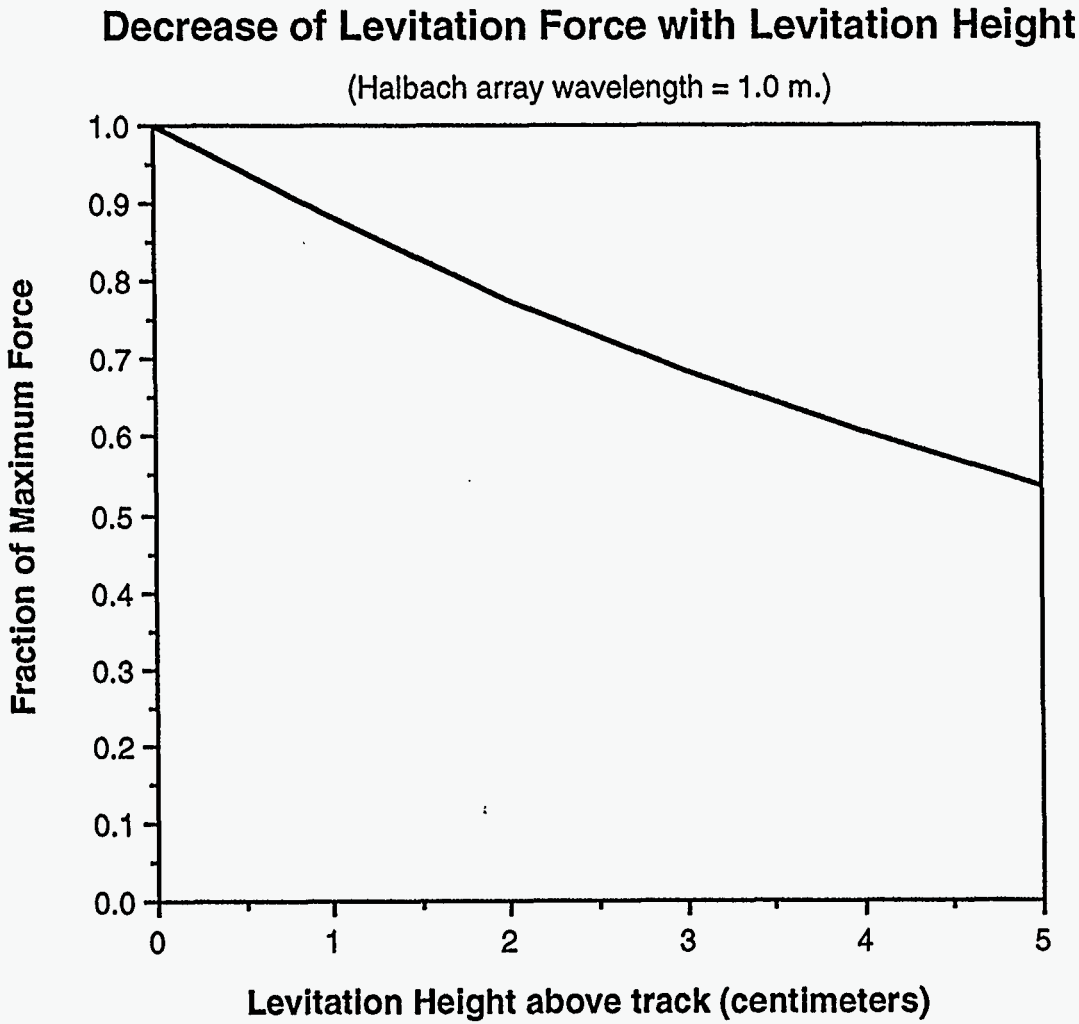
Decrease of Levitation Force with Levitation Height
(Halbach array wavelength = 1.0 m.)
Fraction of Maximum Force
1.0
0.9
0.8
0.7
0.6
0.5
0.4
0.3
0.2
0.1
0.0
0
1
2
3
4
5
Levitation Height above track (centimeters)

Figure 12

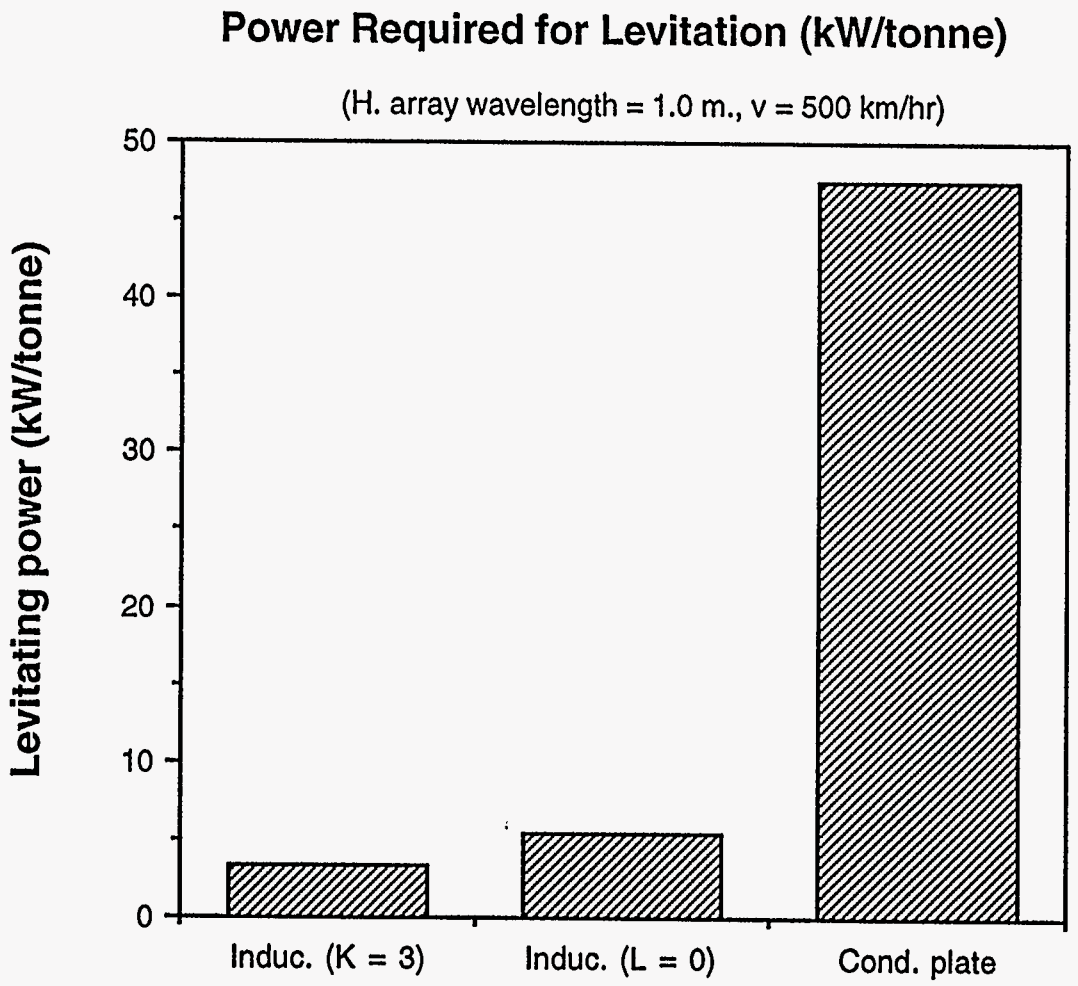
Power Required for Levitation (kW/tonne)
(H. array wavelength = 1.0 m., v = 500 km/hr)
Levitating power (kW/tonne)
50
40
30
20
10
0
Induc. (K = 3)
Induc. (L = 0)
Cond. plate

Figure 13

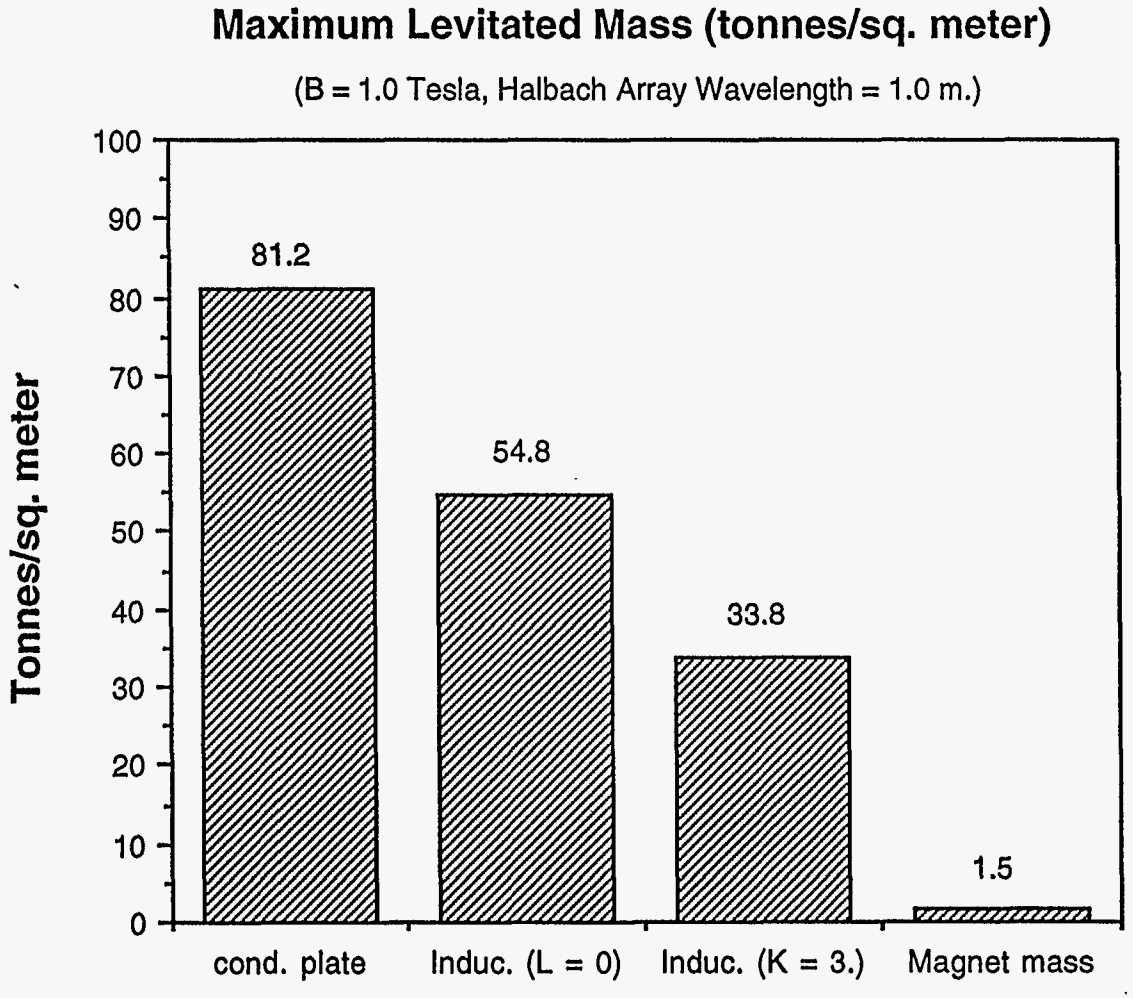
Maximum Levitated Mass (tonnes/sq. meter)
(B = 1.0 Tesla, Halbach Array Wavelength = 1.0 m.)
Tonnes/sq. meter
100
90
80
70
60
50
40
30
20
10
0
81.2
54.8
33.8
1.5
cond. plate
Induc. (L = 0)
Induc. (K = 3.)
Magnet mass

Figure 14

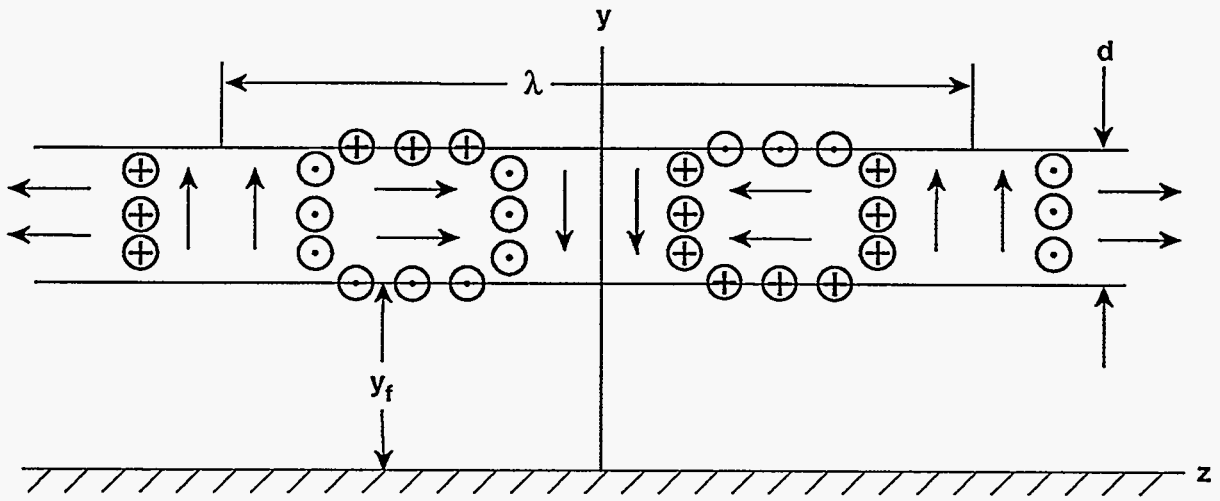

Figure 15

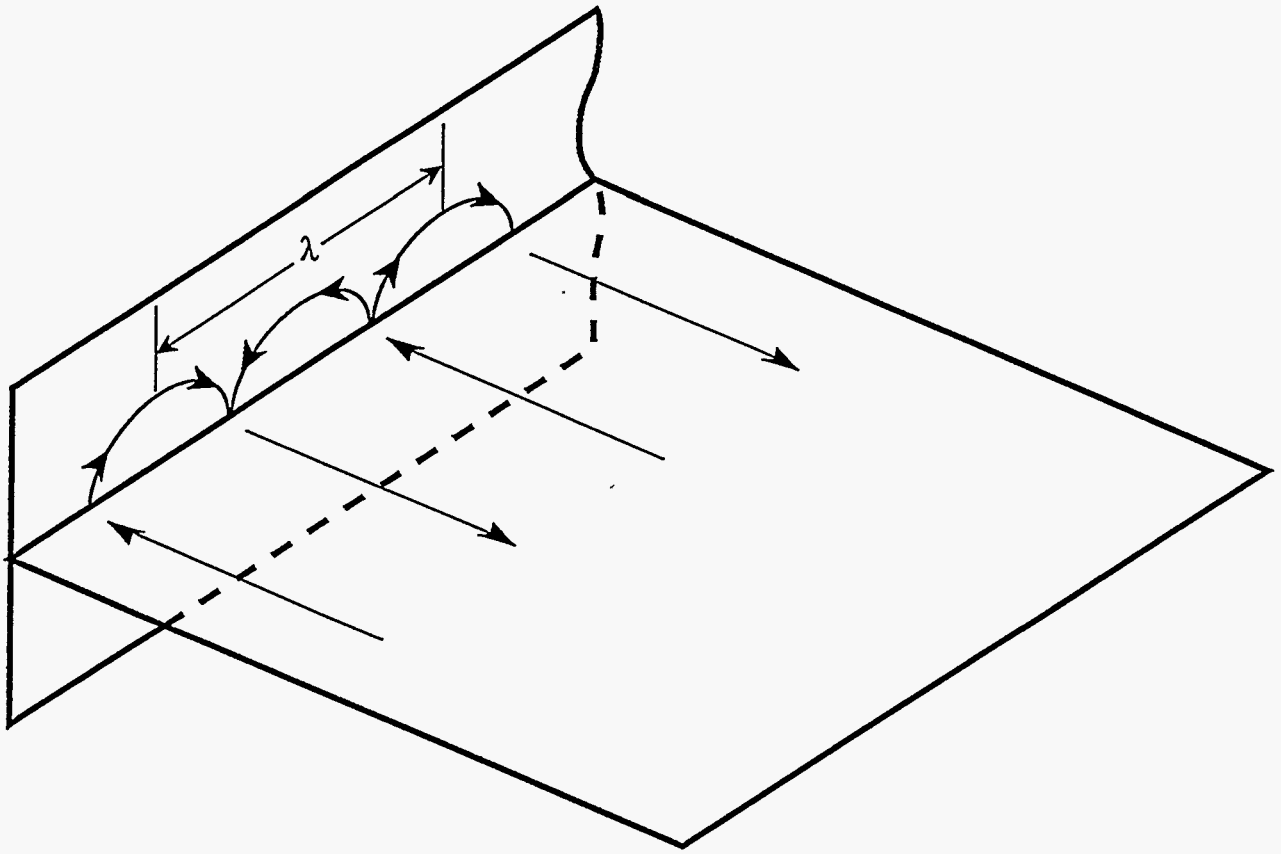

Figure 16

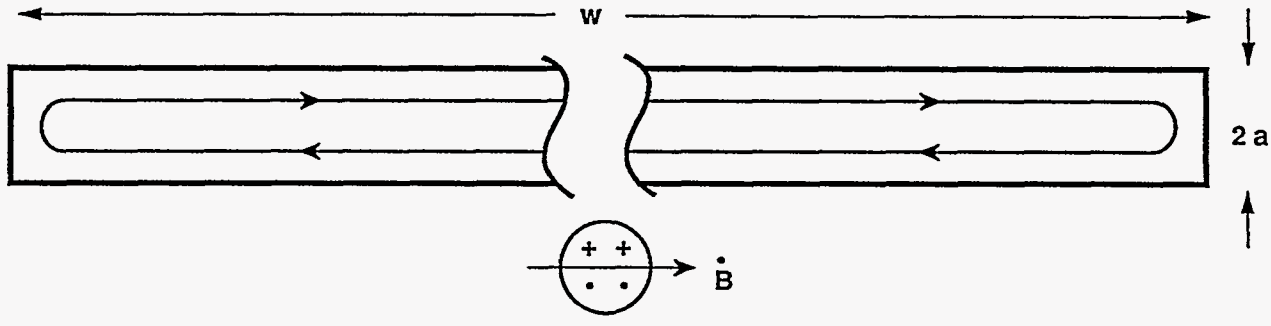

Figure 17

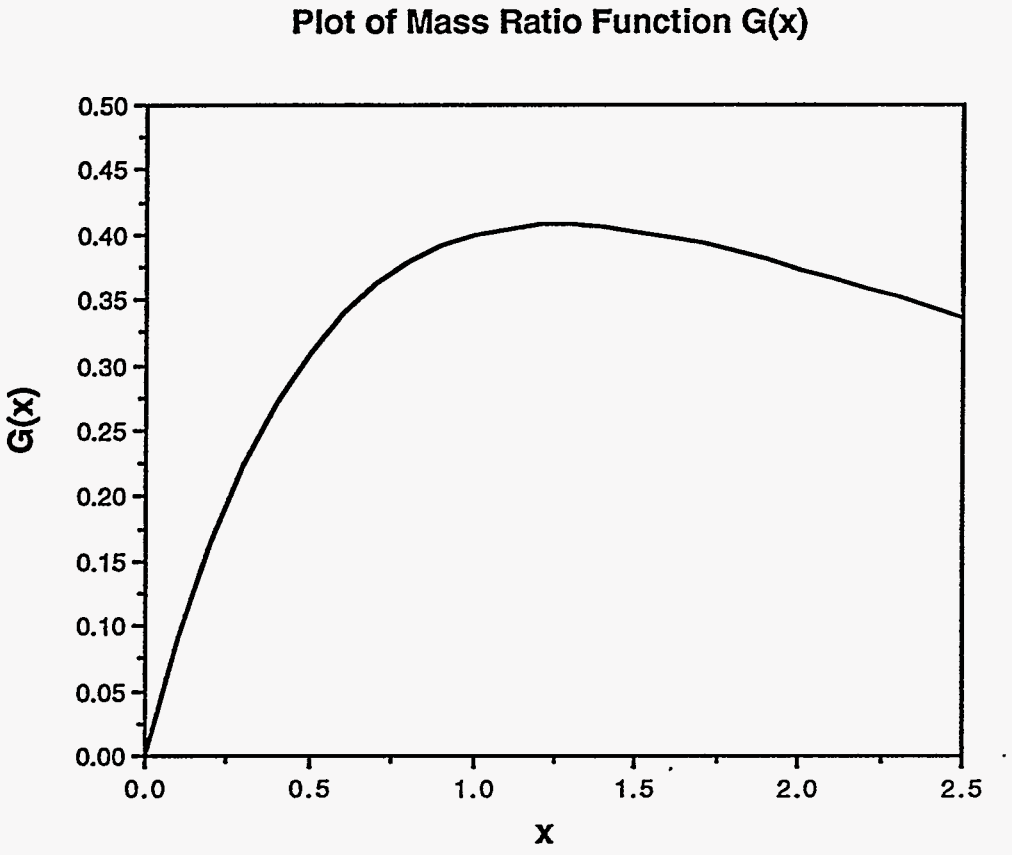
Plot of Mass Ratio Function G(x)
G(x)
0.50
0.45
0.40
0.35
0.30
0.25
0.20
0.15
0.10
0.05
0.00
0.0
0.5
1.0
1.5
2.0
2.5
X

Figure 18

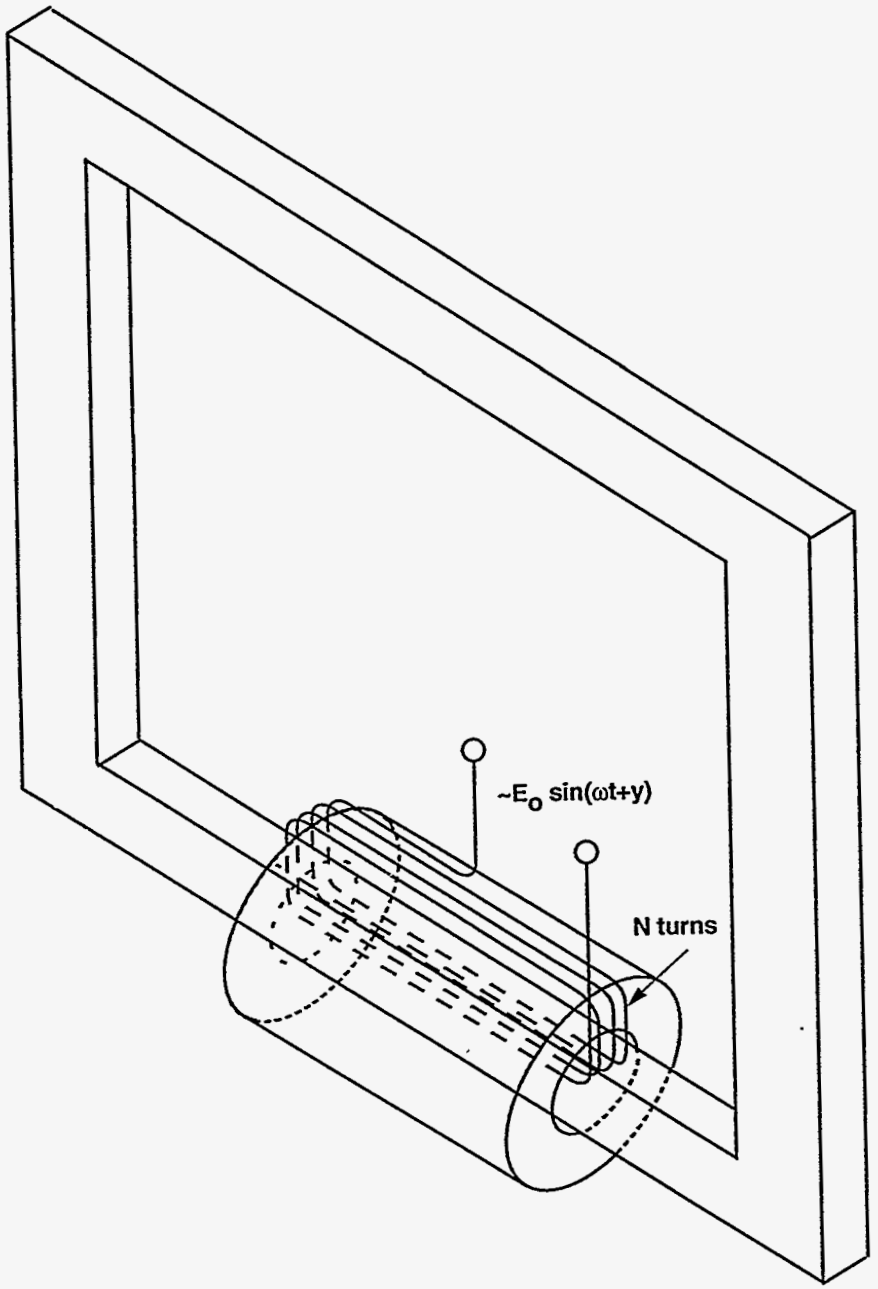

Figure 19

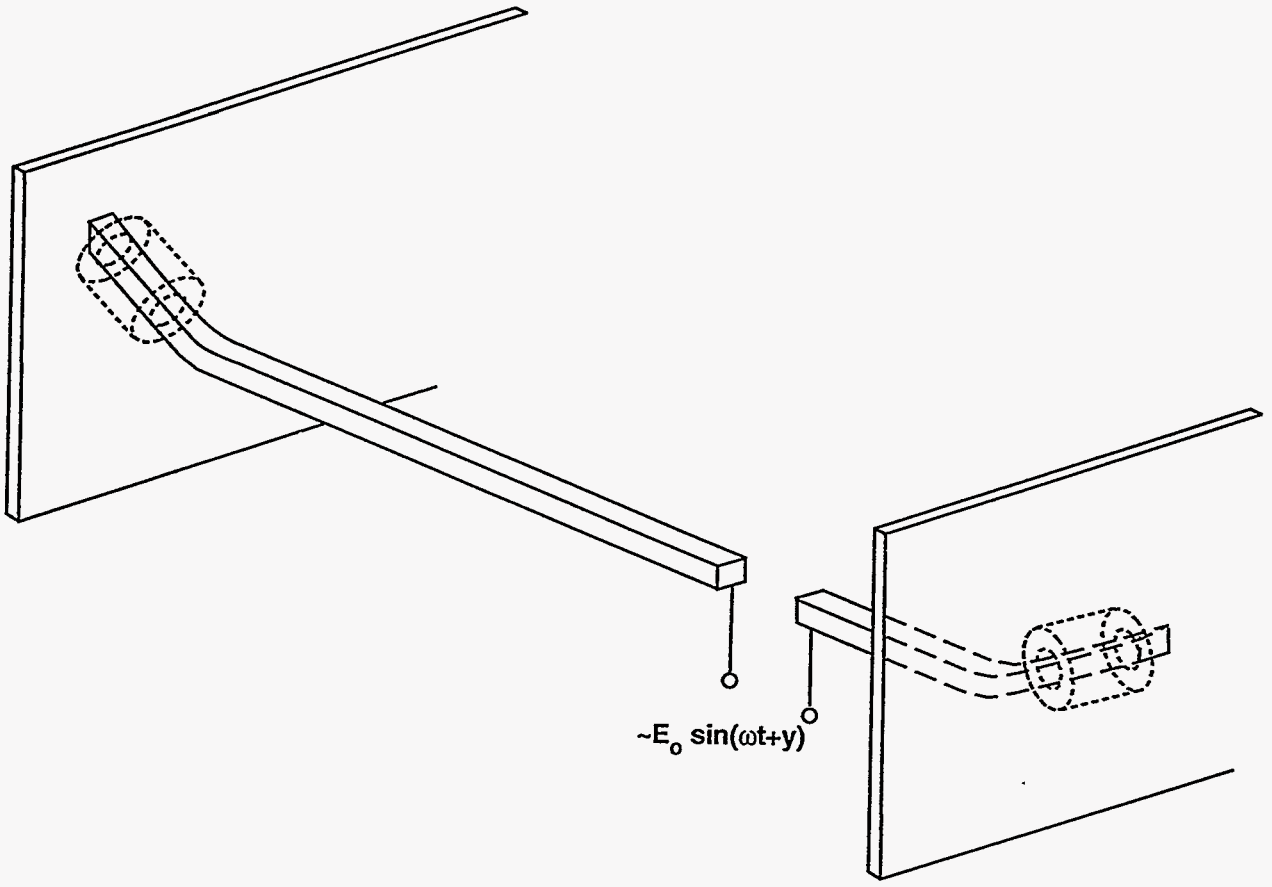

Figure 20

DISCLAIMER

Technical Information Department · Lawrence Livermore National Laboratory
University of California · Livermore, California 94551